COMPUTER INTEGRATED MANUFACTURE OF OPTIMAL B-SPLINE CAMS

by

HOK SIN TEOH

B.S., Kansas State University, 1987

A MASTERS THESIS

submitted in partial fulfillment of the

requirements for the degree

MASTER OF SCIENCE

Department of Mechanical Engineering

KANSAS STATE UNIVERSITY
Manhattan, Kansas

1989

Approved by:

K. Prakash

Major Professor

TABLE OF CONTENTS

LIST OF FIGURES

LIST OF TABLES

ACKNOWLEDGEMENTS

I wish to express my sincere thanks and appreciation to my major advisor, Dr. P. Krishnaswami, for suggesting this research topic, and for his encouragement and assistance.

I would also like to thank Dr. C. L. Huang and Dr. J. G. Thompson for serving on my committee.

Thanks are also due to the National Science Foundation for providing partial support through grant number DMC-8705212.

CHAPTER I

INTRODUCTION

The development of design and analysis techniques for plate cams has remained an active research area for several decades. There are many books devoted entirely to cam design [1, 2], while most machine design books have at least one chapter on this subject. Numerous papers on this topic are still published every year, which indicates that a lot of research still remains to be done in this area.

The use of standard curves is the traditional approach to cam design. The most commonly used curves are harmonic and cycloidal curves. In this approach, the design process is simply the selection of a set of curves which satisfies the required boundary conditions. The process of selecting the curves is a tedious procedure, since different sets of curves are required for different design cases. Moreover, this procedure restricts the range of solutions, since standard curves are only a small subset of the possible solutions which satisfy the specified boundary conditions.

Another common approach in designing cams is to use polynomial curves to represent the cam motions [3]. Depending on the boundary conditions, a polynomial curve with the number of coefficients equal to the number of boundary conditions is generated. Therefore, the solution to a

motion specification is uniquely determined. Obviously, both standard curves and polynomial curves only permit the design to satisfy the boundary conditions; thus the solution may not satisfy other criteria related to performance and manufacture.

An improved approach is presented in [4]. In this case also, polynomial curves are used to design the cam. However, the order of the polynomial curve is set to one order higher than that required to satisfy the boundary conditions. By doing so, a free coefficient is generated, and it is treated as a design variable. This design variable can be used to satisfy performance and manufacturing aspects through an optimization process. More free coefficients can be generated by raising the order of the polynomial curve. However, there is a practical limit on this approach, since a high order polynomial curve causes undesirable oscillations in the cam motion. Besides the limited number of free coefficients, polynomial curves do not provide good local control on cam motion and thus may significantly limit the solution to a design problem. Furthermore, due to the lack of local control, this technique may not be able to provide any solutions for problems where rigorous performance requirements are to be enforced in the interior of a rise or return segment.

The purpose of this work is to present a new design approach which is more powerful than currently available design methods. The approach adopted is to use B-spline curves to design the cam. An example of a B-spline curve is shown in Figure 1.1.

Some preliminary work on the application of B-splines in cam design has been done [5]. However, the overall development in this area is very limited, and automated design procedures are practically non-existent.

B-spline curves are parametric piecewise polynomials which are defined by a series of control points. A B-spline curve provides good local control over its shape. Therefore, it can be used to model a large variety of complex curves, which cannot be modeled by either the standard curves or the polynomials. Since B-splines are conveniently and completely defined by their control points, the design of a B-spline cam is a process of placing the control points at the appropriate locations to meet the specified requirements.

In the current industrial design environment, design tasks are usually performed without considering the relevant manufacturing aspects. Without proper communication between design and manufacture, the solution obtained by this approach may not be one that can be easily produced. Efforts have been made to link the design and manufacturing stages

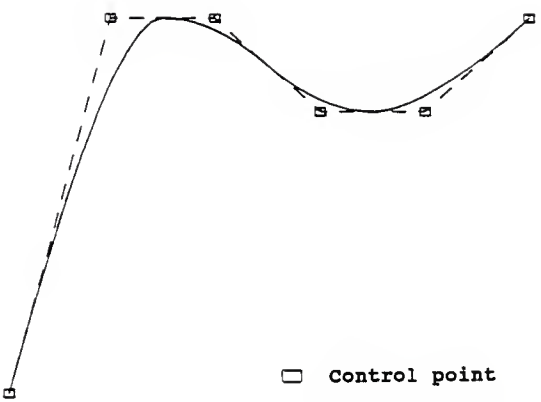

Figure 1.1 : A B-spline Curve

more tightly. These considerations provide a strong motivation to consider both the design and manufacturing aspects simultaneously, so that the final design will satisfy the requirements of both aspects.

In this thesis, a computer-oriented method for integrating the design and manufacture of B-spline plate cams is developed. This approach allows the designer to enforce not only the performance requirements, but also the manufacturing concerns. In this environment, the designer may impose various performance requirements on quantities such as the pressure angle, contact stress, follower acceleration, etc., as well as on manufacturing considerations, such as the cutting time, material, etc. This results in the establishment of a stronger link between design and manufacturing.

In the present work, the linking of design and manufacturing aspects is achieved by using nonlinear optimization techniques. In order to use the techniques of optimal design to solve a given problem, the problem must be stated in a standard format. The format of the standard nonlinear programming problem (NLP) is the following:

Suppose the design of a system is specified by a vector **b** of r design variables:

$$\mathbf{b} = [b1, b2, b3, \ldots, b_r]^T$$

Find the value of **b** to minimize a given cost function, F(b), subjects to the constraints

$$g_j(\mathbf{b}) \leq 0 \qquad j = 1,m$$

$$h_l(\mathbf{b}) = 0 \qquad l = 1,n$$

The advantage of implementing NLP is that it allows integration of design and manufacture. Based on the specified requirements, integration can be achieved by selecting the design variables from both aspects. Similarly, the constraint functions can also be derived from both design and manufacturing. Once the optimization problem is formulated, there are many available algorithms for solving the problem automatically [6, 7]. As a result, implementing NLP in cam designs not only reduces the amount of designer time needed, but also reduces the level of skill required to produce the design.

Two different aspects of manufacturing are considered in this thesis: 1) the cutting time to manufacture the cam, and 2) the material required to produce the cam. In the first case, it is assumed that the cam will be manufactured on an NC machine by an end milling process. It is also assumed that the cam will be cut from a rectangular blank, once the dimensions of the cam are obtained from the optimization procedure. The goal is to design a cam which requires minimum machining time, and satisfies the specified

design requirements. Therefore, the cutting time is considered as the cost function in the NLP. The final design obtained from the optimization process is then utilized to generate the NC codes to produce the cam on an NC machine.

For the second case, we consider the design of a minimum size cam. In this case, the cross-sectional area of the cam is treated as the cost function.

The idea of using optimization techniques in the design of cams is also applicable for problems where manufacturing considerations are not the main concern. The same approach can be extended to problems where the objective function and constraints are all drawn from design considerations.

Note that since B-spline curves are entirely defined by their control points, the coordinates of the points can be treated as design variables in an optimization process for the satisfaction of design requirements. Further discussions on this point are presented in Chapter II and V.

A discussion on the design of cams using B-spline curves is presented in Chapter II. Chapter III is devoted entirely to a discussion of the design aspects, while Chapter IV presents the manufacturing aspects related to plate cams. In Chapter V, the formulation of the nonlinear optimization

problem is presented, with emphasis on the selection of design variables, cost functions and constraint functions. Chapter VI deals with the design sensitivity analysis, while Chapter VII presents some numerical examples that were solved to verify the proposed technique and its implementation. Conclusions drawn from this work and recommendations for future work in this area are summarized in Chapter VIII.

Chapter II

B-SPLINE CAM DESIGN

A variety of mechanical systems are available for use by the designer for the satisfaction of specified motion requirements. The designer must generally choose between constrained linkages, cam systems and control systems. Cam systems are capable of generating a large variety of output motions. The flexibility offered during the design process is one of the key advantages of cam systems [3]. Cams can assume a wide variety of physical shapes, and may drive many different types of followers.

2.1 Types of Cams and Followers

Cams are classified in terms of their physical shape. Figure 2.1 illustrates three different types of cams :

a) A plate cam, also called a radial cam or a disk cam.
b) A wedge cam.
c) A cylindrical cam or barrel cam.

Followers in general may be classified based on one or more of the following criteria:

1) The construction of the surface in contact, e.g., a knife edge, roller, or flat-face.

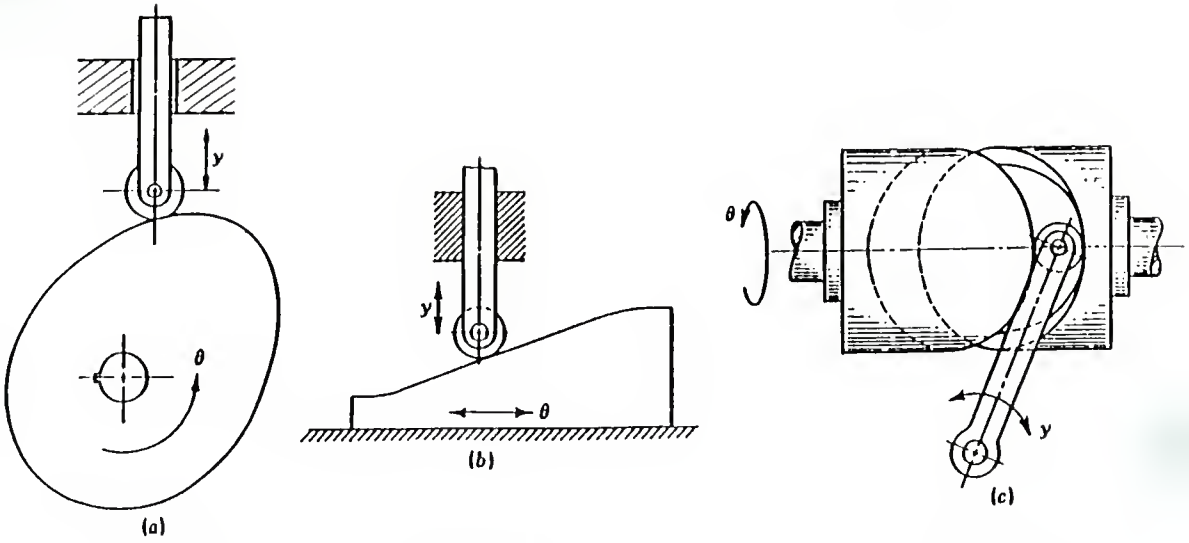

Figure 2.1: Types of Cams

(Extracted from Reference [3])

2) The type of movement, whether translating or oscillating.
3) The location of the line of movement with reference to the cam center, whether radial or offset.

Figure 2.2 shows plate cams with four different types of followers.

This research focuses on plate cam design with offset translating roller follower. Figure 2.3 shows a cam-follower system of this type. In this cam system, the follower translates along its axis, which is displaced from the cam center of rotation.

2.2 Lift Diagram

A cam system is usually driven by an input shaft at a constant velocity to generate the output motion of the follower. The input and output motion of a cam system can be shown on a lift diagram. In Figure 2.4, the abscissa represents one cycle of input motion. The ordinate represents the output motion Y. The output motion can be related to the input motion in functional form :

$$Y = f(\theta) \qquad (2.1)$$

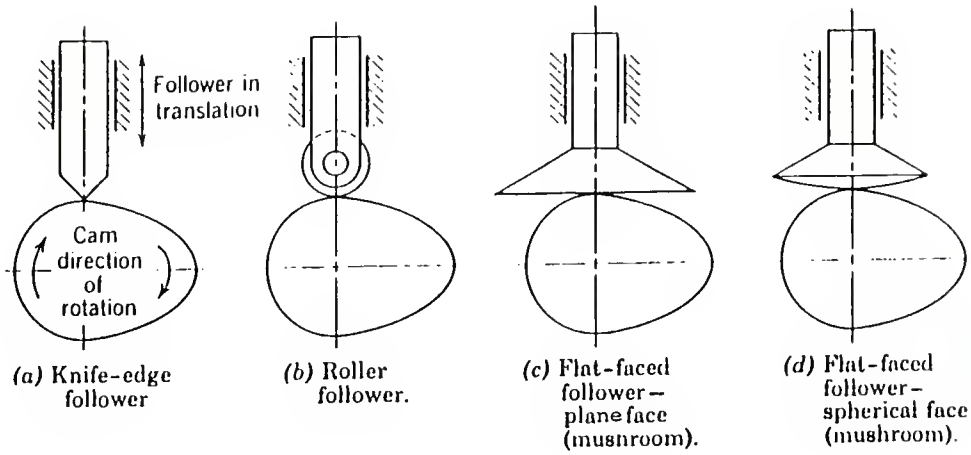

Figure 2.2: Types of Followers

(Extracted from Reference [1])

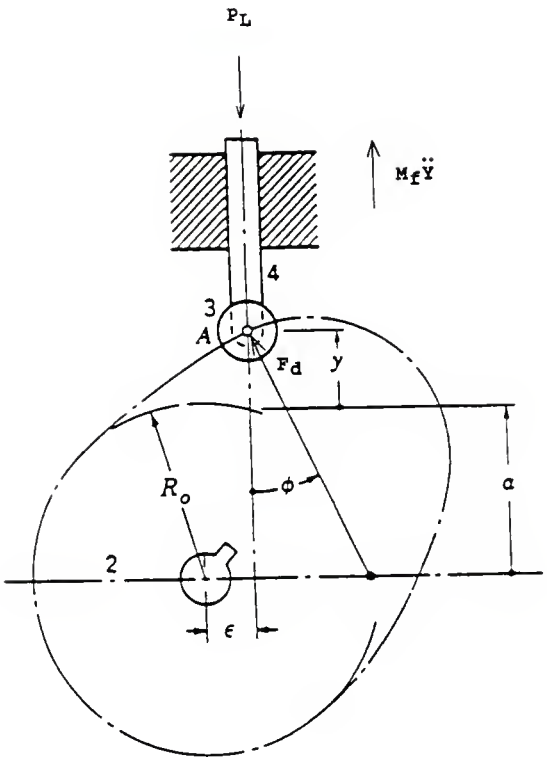

Figure 2.3 : Plate Cam with Offset Translating Roller Follower
(Extracted from Reference [3])

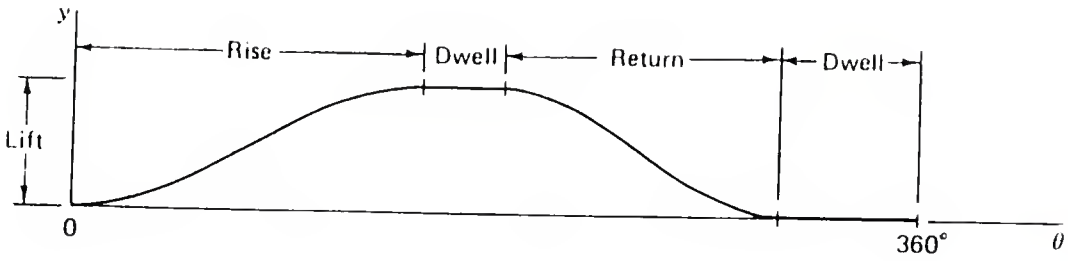

Figure 2.4: Lift Diagram

(Extracted from Reference [3])

where

Y is the follower position

Θ is the cam angle of rotation

The cam motion can be classified into three regions. The region where the follower is moving away from the cam center is called a rise. The maximum rise is called the lift. A return is a region where the follower is moving towards the center of cam. A dwell is a region in which the follower is at rest. In this thesis, it is assumed that the cam motion consists of single rise and single return with top and bottom dwells.

Generally, the follower position is normalized by dividing the actual position, Y, by the total lift. The range of the normalized follower position, denoted by y, is thus from 0 to 1. The actual position can be obtained by multiplying the normalized position by the total lift :

$$Y = L * y \qquad (2.2)$$

where

Y is the actual position

y is the normalized position

Likewise, the derivatives of the follower position with respect to the angle of rotation "θ" are as follows :

$$Y' = L * dy/d\theta \tag{2.3}$$

$$Y'' = L * d^2y/d^2\theta \tag{2.4}$$

$$Y''' = L * d^3y/d^3\theta \tag{2.5}$$

The quantities on the left hand side of Equations (2.3), (2.4) and (2.5) are also known as reduced velocity, reduced acceleration and reduced jerk respectively. The true velocity, acceleration and jerk can be obtained by the following equations :

$$\dot{Y} = Y' * \omega \tag{2.6}$$

$$\ddot{Y} = Y'' * \omega^2 \tag{2.7}$$

$$\dddot{Y} = Y''' * \omega^3 \tag{2.8}$$

where ω is the angular velocity of cam.

2.3 Boundary Conditions

In the last section, it was noted that a complete cycle of the cam motion consists of different zones. When making

the transition from one zone to the next, the designer must ensure continuity of position and its derivatives up to the degree required. This is usually done by specifying appropriate boundary conditions at both ends of the rise and return zones. These boundary conditions are usually specified in terms of normalized position, reduced velocity, reduced acceleration, reduced jerk, etc. Figure 2.5 illustrates the following boundary conditions for a rise zone and a return zone:

Rise Zone

$\theta/\beta = 0$

$$Y = 0, \quad Y' = 0, \quad Y'' = 0, \quad Y''' = 0$$

$\theta/\beta = 1$

$$Y = 1, \quad Y' = 0, \quad Y''' = 0$$

Return Zone

$\theta/\beta = 0$

$$Y = 1, \quad Y' = 0, \quad Y''' = 0$$

$\theta/\beta = 1$

$$Y = 0, \quad Y' = 0, \quad Y'' = 0, \quad Y''' = 0$$

where β is the range of cam rotation for the respective zone.

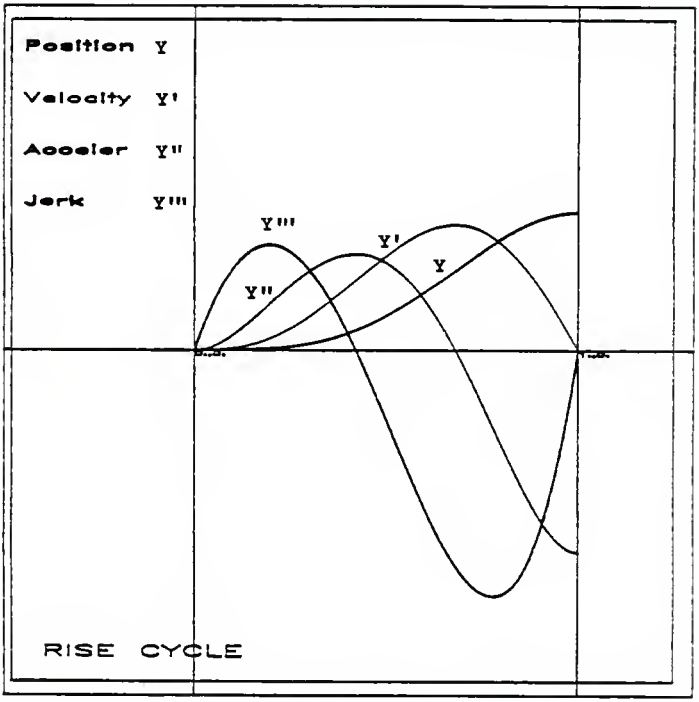

Figure 2.5(a): Illustration of Boundary Conditions for A Rise Cycle
(Extracted from Reference [4])

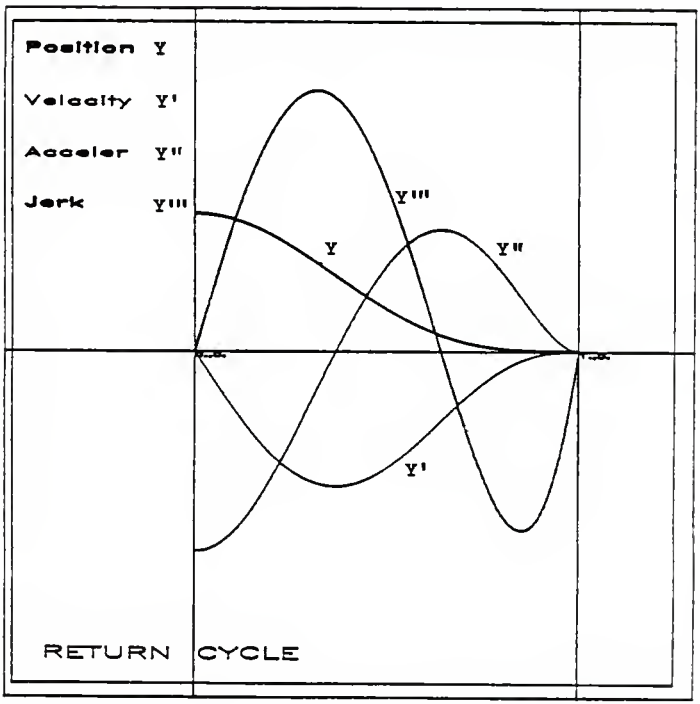

Figure 2.5(b): Illustration of Boundary Conditions for A Return Cycle
(Extracted from Reference [4])

2.4 Techniques of Design

A variety of graphical and analytical techniques are available to design a cam system. In conventional design, basic curves are used to design the cam profile for specified follower motions and boundary conditions. Some of the basic curves that are commonly used are cycloidal curves, simple harmonic curves, modified harmonic curves,parabolic curves, etc. Based on the boundary conditions, the designer must select a set of appropriate curves to meet these conditions. It is obvious that different types of curves are required for different cases. Therefore, designing a cam system using basic curves is a tedious procedure. Furthermore, this technique is purely design for satisfying the boundary conditions. It does not provide any control over the motion in the interior of a region. This may result in serious problems such as excessive pressure angle and stress.

The range of possible solutions can be increased by using polynomials to design the cam profile. This approach can conveniently generate a wide variety of cam profiles, which cannot be modeled using basic curves. To satisfy the boundary conditions, a suitable order of polynomial is required. The designer can generate free variables by raising the order of the polynomial to an order higher than that required to satisfy the boundary conditions [4]. The

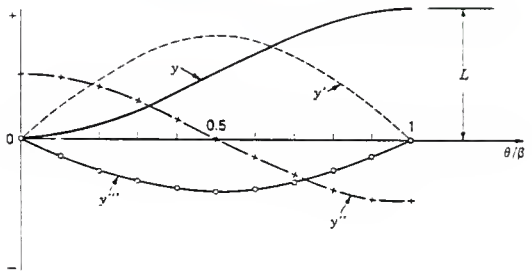

Figure 2.6(a): Displacement Diagram and Derivatives for Full-Rise Simple Harmonic Motion (Extracted from Reference [3])

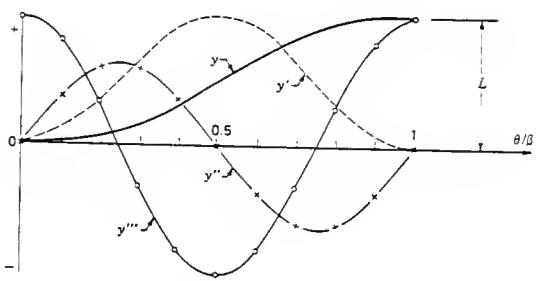

Figure 2.6(b): Displacement Diagram and Derivatives for Full-Rise Cycloidal Motion (Extracted from Reference [3])

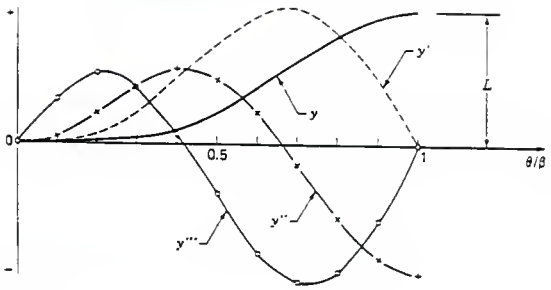

Figure 2.6(c): Displacement Diagram and Derivatives for Full-Rise Modified Harmonic Motion (Extracted from Reference [3])

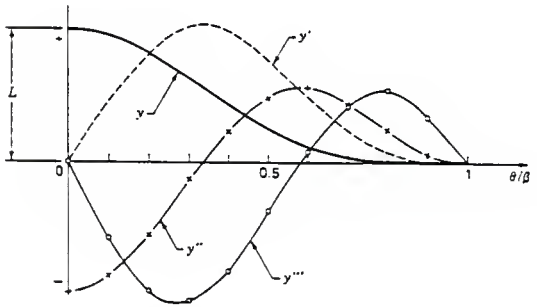

Figure 2.6(d): Displacement Diagram and Derivatives for Full-Return Modified Harmonic Motion (Extracted from Reference [3])

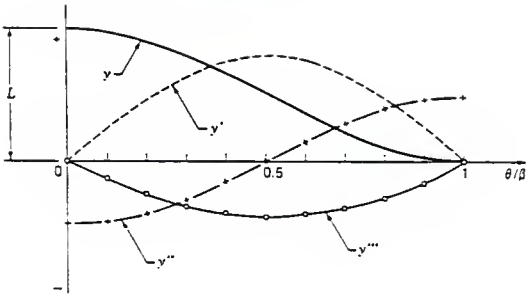

Figure 2.6(e): Displacement Diagram and Derivatives for Full-Return Simple Harmonic Motion (Extracted from Reference [3])

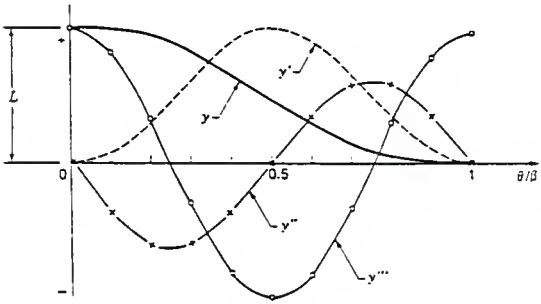

Figure 2.6(f): Displacement Diagram and Derivatives for Full-Return Cycloidal Motion (Extracted from Reference [3])

extra coefficients can be used to satisfy more rigorous constraints, and to reduce cost. However, a very high order polynomial will result in oscillation of the cam profile. Therefore, the designer is restricted to a small number of free variables. Furthermore, due to oscillation, this method may be impractical for design problems with several boundary conditions.

A different approach is adopted in this research. Here, B-spline curves are used to design the cam.

2.5 B-spline Curves

B-spline curves are parametric piecewise polynomials which are defined as follows [8] :

$$P(u) = \sum_{i=0}^{n} P_i \, N_{i,k}(u) \qquad (2.9)$$

where

u is the independent parameter

P_i is the position vector of the i^{th} control polygon vertex

$N_{i,k}(u)$ are blending functions

$P(u)$ is the position vector of the point on the B-spline curve corresponding to a given value of u

For a 2-dimensional problem, $P(u) = [\ P_x(u),\ P_y(u)\ ]$, and $P_i = [\ P_{ix},\ P_{iy}\ ]$.

The blending functions, $N_{i,k}(u)$ are defined recursively by the following equations :

$$\begin{aligned} N_{i,1}(u) &= 1 \quad \text{if } t_i \le u \le t_{i+1} \\ &= 0 \quad \text{otherwise} \end{aligned} \tag{2.10}$$

and

$$N_{i,k}(u) = \frac{(u - t_i)\ N_{i,k-1}(u)}{t_{i+k-1} - t_i} + \frac{(t_{i+k} - u)\ N_{i+1,k-1}(u)}{t_{i+k} - t_{i+1}} \tag{2.11}$$

The t_i are called the knots of the B-spline. They represent the values of the independent variable, u at which the curve switches from one parametric polynomial to the next. For a uniform, non-periodic B-spline, the knots are evenly spaced and defined as follows:

$$\begin{aligned} t_i &= 0 && \text{if } i < k \\ t_i &= i - k + 1 && \text{if } k \le i \le n \\ t_i &= n - k + 2 && \text{if } i > n \end{aligned} \tag{2.12}$$

with $0 \le i \le n + k$

The range of the parameter u is $0 \leq u \leq n - k + 2$. In this evaluation, the convention $0/0 = 1$ is assumed.

The derivatives of B-spline curves are given as follows :

First Derivative

$$P'(u) = \sum_{i=0}^{n} P_i \, N_{i,k}'(u) \tag{2.13}$$

where

$$N_{i,1}'(u) = 0 \tag{2.14}$$

$$N_{i,k}'(u) = \frac{N_{i,k-1}(u) + (u - t_i) \, N_{i,k-1}'(u)}{t_{i+k-1} - t_i} + \frac{(t_{i+k} - u) \, N_{i+1,k-1}'(u) - N_{i+1,k-1}(u)}{t_{i+k} - t_{i+1}} \tag{2.15}$$

Second Derivative

$$P''(u) = \sum_{i=0}^{n} P_i \, N_{i,k}''(u) \tag{2.16}$$

where

$$N_{i,1}''(u) = 0 \tag{2.17}$$

$$N_{i,2}''(u) = 0 \tag{2.18}$$

$$N_{i,k}''(u) = \frac{2 * N_{i,k-1}'(u) + (u - t_i)\, N_{i,k-1}''(u)}{t_{i+k-1} - t_i} + \frac{(t_{i+k} - u)\, N_{i+1,k-1}''(u) - 2 * N_{i+1,k-1}'(u)}{t_{i+k} - t_{i+1}} \tag{2.19}$$

Third Derivative

$$P'''(u) = \sum_{i=0}^{n} P_i\, N_{i,k}'''(u) \tag{2.20}$$

where

$$N_{i,1}'''(u) = 0 \tag{2.21}$$

$$N_{i,2}'''(u) = 0 \tag{2.22}$$

$$N_{i,3}'''(u) = 0 \tag{2.23}$$

$$N_{i,k}'''(u) = \frac{3 * N_{i,k-1}''(u) + (u - t_i)\, N_{i,k-1}'''(u)}{t_{i+k-1} - t_i}$$

$$+ \frac{(t_{i+k} - u)\, N_{i+1,k-1}'''(u) - 3 * N_{i+1,k-1}''(u)}{t_{i+k} - t_{i+1}} \qquad (2.24)$$

In general, the derivative of degree d of a B-spline is

$$p^d(u) = \sum_{i=0}^{n} P_i N_{i,k}^d(u) \qquad (2.25)$$

where

$$N_{i,j}^d(u) = 0 \quad , \quad j = 1, 2, \ldots, d \qquad (2.26)$$

$$N_{i,k}^d(u) = \frac{d * N_{i,k-1}^{(d-1)}(u) + (u - t_i)\, N_{i,k-1}^d(u)}{t_{i+k-1} - t_i}$$

$$+ \frac{(t_{i+k} - u)\, N_{i+1,k-1}^d(u) - d * N_{i+1,k-1}^{(d-1)}(u)}{t_{i+k} - t_{i+1}} \qquad (2.27)$$

2.6 B-spline Cams

As discussed in Section 2.4, conventional design methods use either standard curves or polynomials to represent the cam motion. These curves are usually defined in non-parametric form.

The design approach taken in this work is to use B-splines to represent the lift diagram and to use this representation in the design of the cam. Since B-splines are parametric curves, normalized lift as well as the cam rotation now become functions of the independent B-spline parameter "u":

$$\theta = \sum_{i=0}^{n} P_{ix} N_{i,k}(u) \tag{2.28}$$

$$y = \sum_{i=0}^{n} P_{iy} N_{i,k}(u) \tag{2.29}$$

where

$P_{i,y}$ are the y-coordinates of the control points

$P_{i,x}$ are the θ-coordinates of the control points

Consequently, the true lift of the follower is also a function of u:

$$Y = L * \sum_{i=0}^{n} P_{iy} N_{i,k}(u) \tag{2.30}$$

In the design of conventional cams, the lift is generally treated as an explicit non-parametric function of cam rotation; it is clear from the above equations that this ap-

proach has to be modified in the case of B-spline curves. Here, we must treat both lift and cam rotation as being functions of the parameter u in all derivations.

In addition to the cam angle of rotation and lift, their derivatives must be also taken into consideration. The derivatives of Equations (2.28) and (2.30) can be expressed as follows:

$$d\theta/du = \sum_{i=0}^{n} P_{ix} N_{i,k}'(u) \tag{2.31}$$

$$dY/du = L * \sum_{i=0}^{n} P_{iy} N_{i,k}'(u) \tag{2.32}$$

$$d^2\theta/du^2 = \sum_{i=0}^{n} P_{ix} N_{i,k}''(u) \tag{2.33}$$

$$d^2Y/du^2 = L * \sum_{i=0}^{n} P_{iy} N_{i,k}''(u) \tag{2.34}$$

$$d^3\theta/du^3 = \sum_{i=0}^{n} P_{ix} N_{i,k}'''(u) \tag{2.35}$$

$$d^3Y/du^3 = L * \sum_{i=0}^{n} P_{iy} N_{i,k}'''(u) \tag{2.36}$$

Reduced velocity, reduced acceleration and reduced jerk are given by the following equations:

$$dY/d\theta = (dY/du)/(d\theta/du) \tag{2.37}$$

$$d^2Y/d\theta^2 = \frac{(d\theta/du)*(d^2Y/du^2) - (dY/du)*(d^2\theta/du^2)}{(d\theta/du)^3} \tag{2.38}$$

$$d^3Y/d\theta^3 = \frac{(d\theta/du)*(d\theta/du * d^3Y/du^3 - dY/du * d^3\theta/du^3)}{(d\theta/du)^5} - \frac{3*d^2\theta/du^2 \ (\ d\theta/du * d^2Y/du^2 - dY/du * d^2\theta/du^2)}{(\ d\theta/du \ )^5} \tag{2.39}$$

2.7 Boundary Conditions for B-spline Cams

In this work, it is assumed that the cam consists of a single rise and a single return, with the boundary conditions specified below:

Rise Zone

$\theta/\beta = 0$

$Y = 0 \ , \ Y' = 0 \ , \ Y'' = 0 \ , \ Y''' = 0$

$\theta/\beta = 0$

$Y = 1 \ , \ \ Y' = 0 \ , \ Y'' = 0 \ , \ Y''' = 0$

Return Zone

$\theta/\beta = 0$

$Y = 0 \ , \ Y' = 0 \ , \ Y'' = 0 \ , \ Y''' = 0$

$\theta/\beta = 0$

$Y = 1 \ , \ \ Y' = 0 \ , \ Y'' = 0 \ , \ Y''' = 0$

The remaining of this section is devoted to a discussion on the satisfaction of these conditions. It is to be noted that the implementation of B-splines is also applicable for cams with different boundary condition specifications.

The approach adopted in this thesis is to use one B-spline curve to represent the rise curve and one B-spline curve to represent the return curve. The number of control points used for each of these B-splines is 11. Some of the coordinates of these points may be determined by the specified boundary conditions. The relationship between the boundary conditions and the control points is discussed in the next section.

2.7.1 Position boundary conditions

As shown in Figure 1.1, a B-spline curve passes through both end control points. In a rise zone, position boundary conditions can be satisfied by setting the coordinates of both end points equal to the coordinates of the ends of the rise cycle. For example, if the left end of the rise is at (0,0) and the right end is at (π,1), the first control point must be set at (0,0), and the last control point at (π,1). A similar approach is applicable for the return cycle. In this way, the position boundary conditions at the end points of each cycle are satisfied.

2.7.2 Derivative boundary conditions

For any non-periodic B-spline, the curve is tangent to the first and last spans of the control polygon at the first and last control points. This characteristic can be used to satisfy the first derivative boundary conditions. In order to ensure zero velocity boundary conditions, the tangent of the curve at the appropriate boundary must be set to zero. With reference to Figures 2.7(a) and 2.7(b), this can be achieved by setting the y-coordinates of control points P_1 and P_9 equal to the y-coordinate of the first and the last

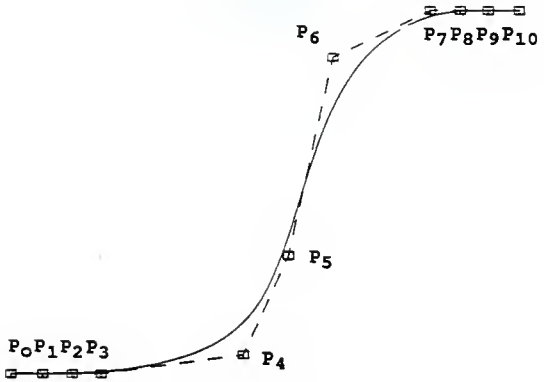

Figure 2.7(a) : A Rise Cycle B-spline

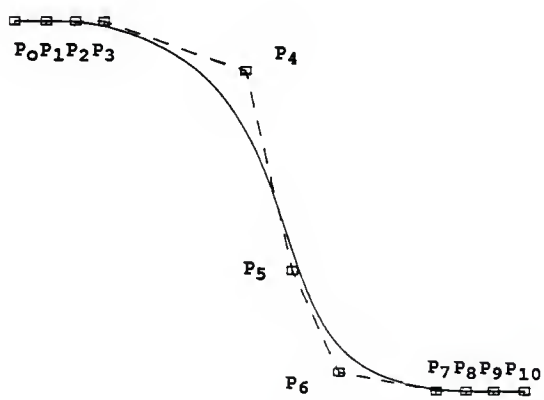

Figure 2.7(b) : A Return Cycle B-spline

points respectively. A similar approach can be applied to acceleration and jerk boundary conditions. To obtain zero acceleration and jerk at both boundaries, the y-coordinates of points P_2 and P_3 must be set equal to the y-coordinate of point P_0, while the y-coordinates of points P_7 and P_8 must be set equal to y-coordinate of point P_{10}. As a result of imposing the boundary conditions, the x-coordinates of points P_0 and P_{10}, and the y-coordinates of points P_1, P_2, P_3, P_7, P_8, and P_9 are fixed. The x-coordinates of points P_1, P_2, P_3, P_4, P_5, P_6, P_7, P_8 and P_9, and the y-coordinates of points P_4, P_5 and P_6 are free variables. They are used as design variables to satisfy constraints and to reduce cost in an optimization process.

2.8 Advantages of B-spline Curves

B-spline curves possess several properties which make them very attractive for cam design applications.

a) Degree of continuity : The degree of continuity of a B-spline curve is controlled only by the parameter k. With a specified value of k, the continuity of the curve is (k-2). Therefore, the desired degree of continuity can be obtained by setting k to an appropriate value. For example, if continuity up to jerk is required, the value of k must be at least 5. In this work, the value of k is set to 5.

b) Flexible number of control points: As noted earlier, the number of control points used in this work is 11. The boundary conditions impose restrictions on the coordinates of some of the control points, while the remaining coordinates can be treated as design variables. B-spline curves can be extended to have more control points without affecting local properties. As a result, more points can be added to provide more design variables to satisfy more rigorous performance requirements.

c) Good local control: B-splines provide good local control. Local control is the ability to change a certain section of a curve without affecting the shape of the curve far away from the region of change. As shown in Figure 2.8, the location of control point P_5 is shifted to a new position at P_5^*. The effect of shifting the point changes only a small neighboring section of the curve. This indicates that B-spline curves provide good local control. Such control plays an important role in the design of cams. Very often, only a few sections of the profile of the initial design violate the design requirements. It is therefore desirable to retain the sections with no violation, and correct only the problem regions. This is

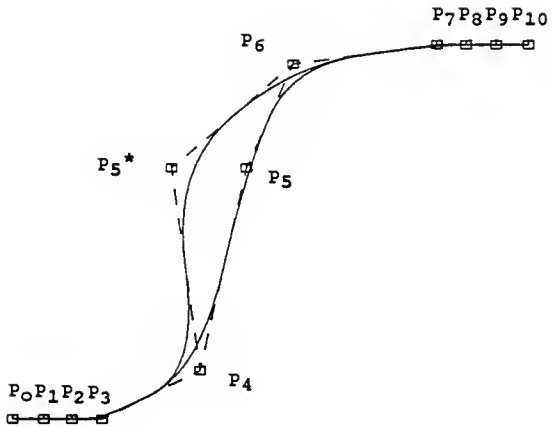

Figure 2.8: Illustration of Local Control

not possible if either standard curves or polynomials are used, since they do not provide local control. By using B-splines, the violation may be reduced or eliminated by shifting the control points near the problem regions appropriately, while retaining the shape of the curve at other regions where no violation occurs.

CHAPTER III

DESIGN CONSIDERATIONS

For a cam design to be acceptable, it must satisfy a specified set of performance requirements. Therefore, it is necessary to establish a set of design relationships to account for these requirements. These performance requirements are enforced in the optimization process as constraints. The design requirements considered in this thesis are pressure angle, separation, oscillation, stress and undercutting. The details of these considerations are discussed below. Other design considerations are treated as problem dependent, with the designer being allowed to add as many other performance constraints as required.

3.1 Pressure Angle

The pressure angle is the angle between the normal to the pitch curve and the axis of the follower stem. The value of the pressure angle should be kept low to reduce friction and chattering of the follower, as well as to obtain better force transmission [1]. From Figure 2.3, we observed that only the force component along the axis of the follower is used to overcome the output load. The tangential component of the force causes friction between the follower stem and its guideway. Therefore, a smaller pres-

sure angle provides better force transmission, and increases the smoothness of the follower motion.

Designers often limit the pressure angle to a maximum of 30°. However, if the follower bearings are good and the cam follower is rigid, the maximum pressure angle may be increased to a larger value.

In Figure 2.3, using the Aronhold-Kennedy theorem of three centers, the instantaneous center of velocity between cam 2 and follower 4 is at P_{24}. Since the follower is translating, all points of the follower have velocity equal to that of P_{24}, which is also equal to the velocity of the coincident point on link 2 [3].

$$V_P = \dot{Y} = \omega * R_P \tag{3.1}$$

where

ω is the angular velocity of cam

R_P is the distance between cam center of rotation and point P_{24}

Dividing equation (3.1) by ω, the equation is reduced to

$$\dot{Y}/\omega = Y' = R_P = e + (a + Y) \tan(\phi) \tag{3.2}$$

where a is the vertical distance from the cam axis to the prime circle and is given by

$$a = \text{sqrt}(R_o^2 - e^2) \tag{3.3}$$

where

R_o is base radius of the cam

e is the follower offset.

The final expression for pressure angle is given by :

$$\phi = \tan^{-1} \frac{Y' - e}{\text{sqrt}(R_o^2 - e^2) + Y} \tag{3.4}$$

3.2 Separation

The cam and the roller follower must maintain continuous contact at all times. Failure to maintain continuous contact between the cam and the follower will result in separation. This is generally undesirable since the motion generated by the roller follower may be unacceptable. In addition, separation may cause other problems such as impact between the follower and cam surface, wear, noise, etc. To avoid separation, we examine the dynamics of the cam system. As shown in Figure 2.3, the driving force of the cam is given by

$$F_d = (P_L + M_f * \ddot{Y})/\cos(\phi) \tag{3.5}$$

where

P_L is the preload specified by the user (including friction, spring force, etc.)

M_f is the mass of the follower mechanism

$\ddot{Y}$ is the true acceleration of the follower

The force F_d must always maintain a positive value for continuous contact between the cam and the follower. However, if the acceleration required to track the cam is too high on the return cycle, a negative value of F_d is required to maintain contact. Since this is physically impossible, it will result in separation between the cam surface and the follower.

To prevent separation, one option is to increase the preload [2]. However, an increase in the preload will increase the contact stress between the cam and the follower. A second alternative is to keep the acceleration during the return cycle to a minimum by controlling the shape of the profile. In this thesis, separation between the follower and the cam is avoided by imposing a constraint in the optimization process, which restricts the driving force to be positive throughout the motion.

3.3 Elimination of Oscillation in the Follower Velocity

Oscillation is a condition in which the follower attempts to descend during the rise cycle, or ascend during the return cycle. Due to oscillation, it is possible that in the interior of a rise or a return, the follower may attempt to move to a location beyond the specified lower or upper boundary limits. This is unacceptable and should be avoided, since the cam system may be confined within a limited space and movements beyond the limits may cause severe damage to the system. Therefore, it is necessary to design a cam with monotonic ascent during the rise and monotonic descent during the return to avoid oscillation.

In this work, monotonic ascent during the rise and monotonic descent during the return are obtained by restricting the velocity of the cam follower to be positive throughout the rise cycle and negative throughout the return cycle.

3.4 Stress

Stress at the area of contact between the cam and the follower is another important factor. Excessive stress can cause surface wear and failure of the cam system.

According to Hertz [1], the stress distribution of two cylinders in contact, assuming perfect alignment, is rectan-

gular in shape. The maximum compressive stress of two perfectly aligned cylinders is at the center of the contact area and decreases to zero at the ends.

The Hertzian equation to calculate the maximum compressive stress for two cylinders in contact and in alignment is given as follows [1]:

$$S_c^2 = \frac{F_d \left(r_c + r_f \right)}{\pi * t_c * r_f * r_c * ((1-\mu_c^2)/E_c + (1-\mu_f^2)/E_f)} \qquad (3.6)$$

where

S_c = Maximum compressive stress at any point, lb/in.^{2}

F_d = normal load on cam profile, lb.

r_c and r_f = radii of curvature of cam and follower respectively, in.

t_c = thickness of contacting cam and follower

μ_c and μ_f = Poisson's ratio for cam and follower respectively.

E_c and E_f = moduli of elasticity of cam and follower, respectively.

3.5 Undercutting

The radius of curvature of the cam profile is another important consideration in the design of the cam. An adequate cam curvature is required to produce correct follower movement. If the curvature of the cam is too sharp, the follower may not be able to trace the profile correctly, and thus the motion generated may be unacceptable. In addition, a sharp curvature may cause excessive stress on the cam surface, which may cause wear and eventual failure of the system. This condition is called undercutting.

With a roller follower, undercutting occurs in a convex curve when the radius of curvature of the pitch curve is less than the radius of the roller. With a concave curve, it occurs when the radius of curvature of the pitch curve is less than zero or the radius of curvature of the cam profile is less than the radius of the roller. Figure 3.1 illustrates the problems of undercutting. For a safe design, the curvature of the profile must be greater than one and a half times the radius of the follower [9]. The equation for the radius of curvature is given as follow :

$$r_c = \frac{(c^2 + (Y' - e)^2)^{3/2}}{c^2 + (Y' - e)\ (2*Y' - e) - c*Y''} \qquad (3.7)$$

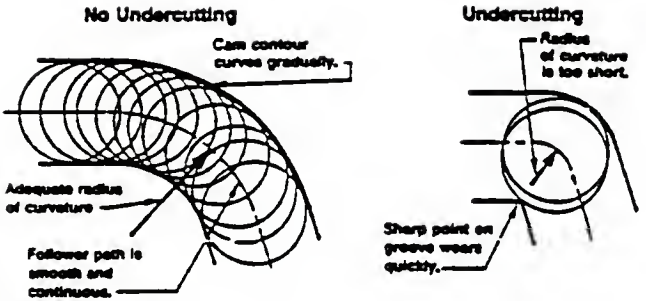

Figure 3.1 : Illustration of Undercutting
(Extracted from Reference [14])

where

c is the distance between cam center and cam profile, given by

$$c = a + Y \tag{3.8}$$

Undercutting can be avoided by either or both of the following ways :

1) Use a small roller. However, a small roller size may cause excessive stress in the roller.
2) Use a larger cam. This approach generally has a practical limitation, since a larger cam increases space requirements, material cost, etc.

In this thesis, the radius of the follower is kept constant; therefore undercutting is to be avoided by properly sizing the cam.

The considerations that have been described are enforced as constraints in the optimization process as described in Chapter V.

CHAPTER IV

MANUFACTURING ASPECTS

In this research, our purpose is to simultaneously consider the design and manufacturing aspects in order to design cams with the lowest manufactured cost or lowest cutting time. For designing cams with low machining time, a mathematical model for estimating the cutting time must first be derived. The relevant equations for estimating the cutting time are discussed later in this chapter. For minimizing the manufactured cost, we consider the cost of the metal required to make the cam to be the most significant contributor to the total cost. Since cams with smaller size require less material, it follows that a minimum size cam minimizes the total cost.

4.1 Cutting Time

There are a variety of ways to manufacture plate cams. One possibility is the use of numerically controlled milling machines, which offer significant benefits in terms of speed, reliability and accuracy. The use of NC machines requires the process planner to generate data points for the tool path. Today, with the aid of digital computers, the data points for the tool path can be generated conveniently,

and then transferred to a tape and fed into the NC machine. In the present work, we consider manufacture of the cam using a Pratt & Whitney Tapemate Series C NC milling machine. This is a bed-type vertical milling, drilling and tapping machine with a 7-tool turret. The machining method selected to manufacture the cam is the end milling slotting process. Once the geometry of the cam is decided by the optimization process, a blank is then cut to the desired geometry and shape.

During the manufacturing process, it is necessary to select a set of machining parameters, such as tool size, spindle speed, etc. These parameters are generally decided based on the engineer's experience. For the purpose of this work, the selection of the necessary machining parameters are made by referring to standard tables [10]. As indicated in Table 1, a tool diameter of 3/4 inches provides a good feed rate for a wide variety of materials. Furthermore, a tool size of 3/4 inches is also the most appropriate considering both tool life and productivity.

The other relevant manufacturing parameters that were selected are listed below:

Tool material ------ High Speed Steel
Tool diameter ------ 3/4 inches
Number of teeth ---- 4

Table 1 : Machining Data for End Milling Process

MATERIAL	HARDNESS BHN	CONDITION	DEPTH* OF CUT inches	SPEED fpm	FEED – Inches per Tooth				HSS TOOL MATERIAL except as noted
					WIDTH OF SLOT – Inches				
					1/4	1/2	3/4	1 to 2	
1. FREE MACHINING CARBON STEELS, WROUGHT Low Carbon Resulfurized 1212 1213 1215	100 to 150	Hot Rolled or Annealed	.250	125	-	-	.0025	.0035	M2, M7
			.050	135	.001	.0015	.002	.005	M2, M7
	150 to 200	Cold Drawn	.250	110	-	-	.0025	.0035	M2, M7
			.050	120	.001	.0015	.002	.003	M2, M7
Low Carbon Resulfurized 1108 1118 1109 1119 1110 1144 1116 1211 1117	100 to 150	Hot Rolled or Annealed	.250	110	-	-	.0025	.003	M2, M7
			.050	120	.001	.0015	.002	.0025	M2, M7
	150 to 200	Cold Drawn	.250	90	-	-	.0025	.003	M2, M7
			.050	100	.001	.0015	.002	.0025	M2, M7
Medium Carbon Resulfurized 1132 1141 1137 1145 1139 1146 1140 1151	175 to 225	Hot Rolled, Normalized, Annealed or Cold Drawn	.250	105	-	-	.0025	.003	M2, M7
			.050	115	.001	.0015	.002	.0025	M2, M7
	275 to 325	Quenched and Tempered	.250	75	-	-	.0025	.003	M2, M7
			.050	85	.001	.0015	.002	.0025	M2, M7
	325 to 375	Quenched and Tempered	.250	45	-	-	.002	0025	M2, M7
			.050	50	.0005	.001	.0015	.002	M2, M7
	375 to 425	Quenched and Tempered	.250	25	-	-	.0015	.002	T15, M33, M41 Thru M47
			.050	30	.0005	.0007	.001	.0015	T15, M55, M41 Thru M47
	100 to 150	Hot Rolled, Normalized, Annealed or Cold Drawn	.250	135	-	-	.0025	.0035	M2, M7
			.050	145	.001	.0015	.002	003	M2, M7
	150 to 200	Hot Rolled, Normalized, Annealed or Cold Drawn	.250	120	-	-	.0025	.0035	M2, M7
			.050	130	.001	.0015	.002	.005	M2, M7
	200 to 250	Hot Rolled, Normalized, Annealed or Cold Drawn	.250	105	-	-	.0025	003	M2, M7
			.050	115	.001	.0015	.002	.0025	M2, M7

(Extracted from Reference [10])

Depth of cut ------- 0.25 inches

Feed per tooth ----- 0.002 inches

Cutting speed ------ 110 feet per minute

Once the cutting speed and tool diameter are known, the spindle speed in RPM can be calculated as follows [11]:

$$V_s = (12 * V_c) / (\pi * d_t) \qquad (4.1)$$

where

V_c is the nominal cutting speed in fpm

d_t is the tool diameter in inches

The Pratt & Whitney machine used in this work has only six spindle speeds. Therefore, the closest lower speed is selected. Using this spindle speed, the actual cutting speed is given by

$$V_{ca} = 12 / (60 * \pi * d_t) * V_s' \qquad (4.2)$$

where

V_{ca} is the actual cutting speed in fpm

V_s' is the actual spindle speed in RPM

Now, the feed in inches per second can be computed as follows:

$$\text{Feed} = \text{fpt} * N_t * V_s'/60 \qquad (4.3)$$

where

fpt is the feed per tooth in inches

N_t is the number of teeth in the tool

4.1.1 Generation of data points

The machining of the cam requires the computation of data points for the tool path. Conventionally, a series of fixed steps is taken along the x-axis and y-axis of the milling machine to generate the cam contour [2]. The size of the steps is determined at the most critical section of the profile, where the step size is required to be sufficiently small to meet the desired accuracy. However, it is possible to use variable step sizes to generate the contour, because at some sections a larger step may be allowed for the same accuracy [4]. The advantage of this approach is that it minimizes the number of turns of the tool path, thus reducing the cutting time significantly.

As shown in Figure 4.2, the data points are restricted

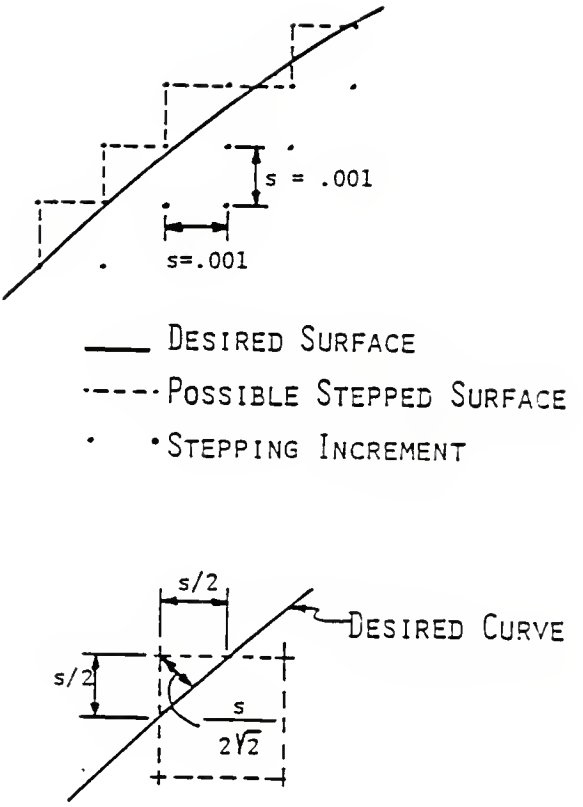

Figure 4.1 : Fixed Step Size Path Generation
(Extracted from Reference [2])

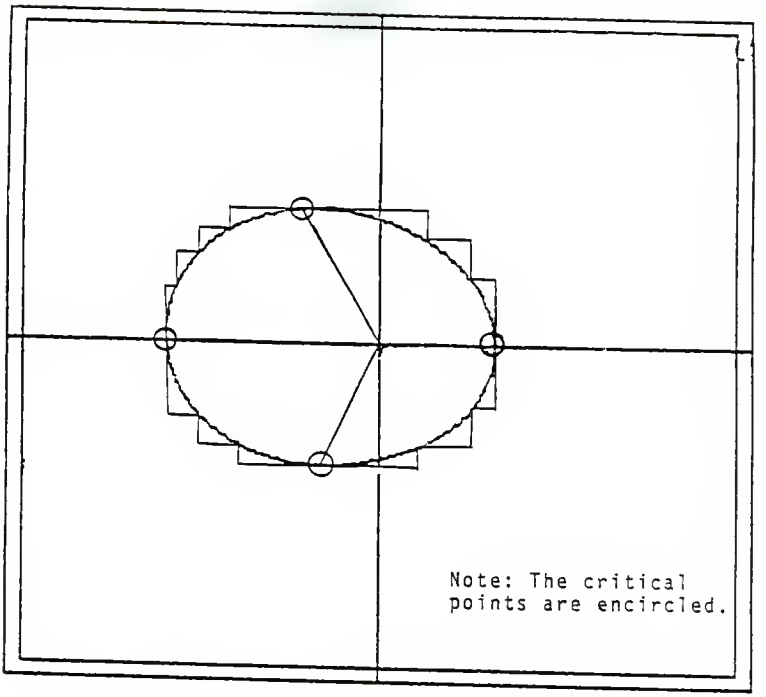

Figure 4.2 : Variable Step Size Path Generation
(Extracted from Reference [4])

to be on the outside of the cam profile. Therefore, the cutter never cuts into the profile, but remains outside within a specified tolerance "ϵ". This strategy will allow subsequent improvement of the surface finish and accuracy of the cam by passing it through a finishing process, such as profile grinding.

The cam motion consists of a rise, a top dwell, a return and a bottom dwell. The approach adopted is to generate data points for each cycle individually. Therefore, the starting point of the tool path corresponding to a cycle is at the start of the cycle, and the ending point of the tool path is at the other end of the cycle.

To generate data points, it is necessary to divide the profile into different sections, based on the sign of the slope dY/dX. This is done by computing the critical points of the profile with respect to the coordinate axes, i.e., points at which the slope is either zero or infinity. Each section is confined between two consecutive critical points as shown in Figure 4.2. Note that the sign of the slope remains the same within a section.

The purpose of dividing the cam profile into different sections is because the sequence of data point generation for a section with positive slope is different from a section with negative slope:

a) Figure 4.3(a) shows a section with positive slope. Starting at point (X_o,Y_o), the tool moves along the x-axis to point (X_1,Y_1), so that the maximum deviation from the profile is equal to the specified tolerance "ϵ". The tool then moves along the y-axis to (X_2,Y_2). Notice that this strategy maximizes the step sizes along each direction, and thus reduces the number of turns in the tool path. This procedure is repeated until the entire section is completed.

b) For a section with negative slope as shown in Figure 4.3(b), starting from (X_o,Y_o), the tool first moves along the y-axis to (X_1,Y_1), and then along the x-axis to (X_2,Y_2).

In computing the data points, since the rise and the return are represented by parametric curves, the process of data point generation for these cycles is different from the process that is used for the dwells.

1) Rise and Return

The process of data point generation is executed as follows:

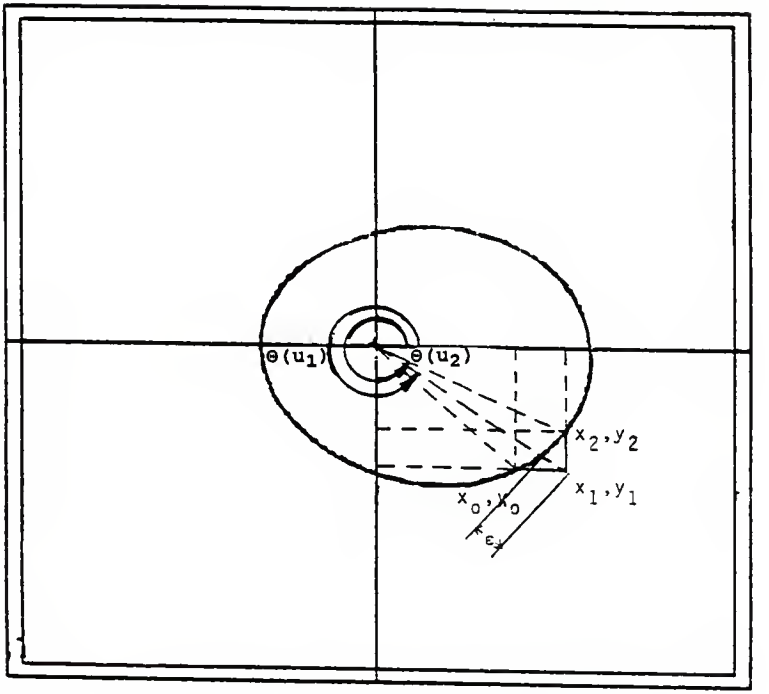

Figure 4.3(a) : Generation of Data Points for a Section with Positive Slope
(Extracted from Reference [4])

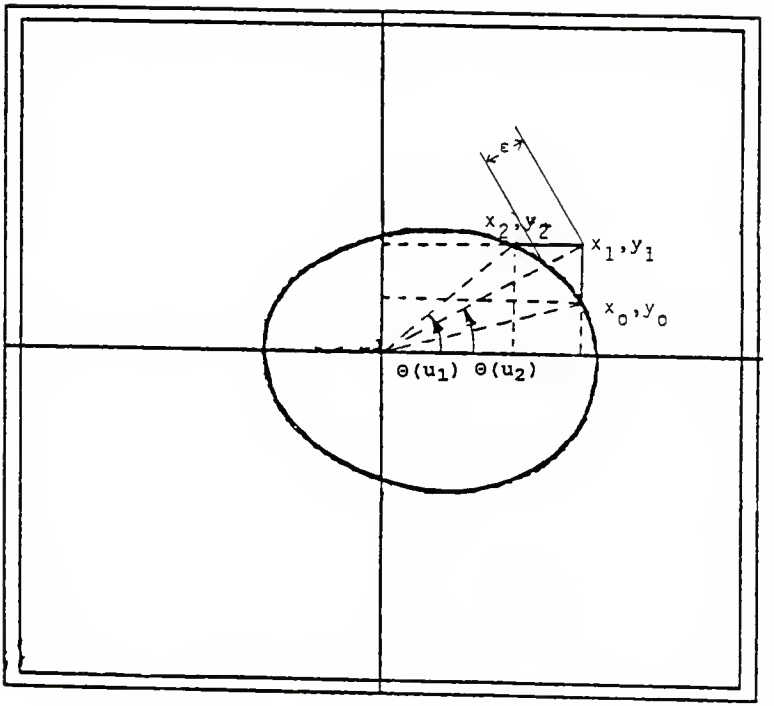

Figure 4.3(b) : Generation of Data Points for a Section with Negative Slope
(Extracted from Reference [4])

a) If $dY/dX > 0$:

Figure 4.3(a) shows a section of profile with positive slope. The geometric relationship between points (X_o, Y_o) and (X_1, Y_1) is given by

$$f(u) = (r(u) + \epsilon) * \sin(\theta(u)) - Y_o = 0 \qquad (4.4)$$

where

$r(u)$ is the instantaneous radial distance to the cam profile

$\theta(u)$ is the angle corresponding to the data point

The equations for $r(u)$ and $\theta(u)$ are given as follows:

$$r(u) = R_o + L * \sum_{i=0}^{n} P_{iy} N_{i,k}(u) \qquad (4.5)$$

$$\theta(u) = \sum_{i=0}^{n} P_{ix} N_{i,k}(u) \qquad (4.6)$$

Similarly, a mathematical expression can be derived from the geometric relationship between points (X_1, Y_1) and (X_2, Y_2):

$$g(u) = r(u) * \cos(\theta(u)) - X_1 = 0 \qquad (4.7)$$

Referring to Figure 4.3(a), suppose that X_o and Y_o are known coordinates, and the angle at this point is also known. To generate the next data point (X_1,Y_1), a Newton-Raphson iteration is implemented to solve Equation (4.4).

$$u_{j+1} = u_j - f(u_j)/f'(u_j) \tag{4.8}$$

where

j is the iteration number

and $f'(u_j)$ is given by

$$f'(u_j) = (r(u_j) + \epsilon) * \cos(\theta(u_j)) * \theta'(u_j) + r'(u_j) * \sin(\theta(u_j)) \tag{4.9}$$

where

$$\theta'(u_j) = \sum_{i=0}^{n} P_{ix} N_{i,k}'(u_j) \tag{4.10}$$

When the parametric value u is known, the coordinates of (X_1,Y_1) are given by

$$X_1 = r(u) * \cos(\theta(u)) \tag{4.11}$$

$$Y_1 = Y_0 \tag{4.12}$$

The next data point to be generated is (X_2, Y_2). The value of the parameter u corresponding to this point can be calculated by the following Newton-Raphson iteration for solving Equation (4.7)

$$u_{j+1} = u_j - g(u_j)/g'(u_j) \tag{4.13}$$

where

j is the iteration number

and $g'(u_j)$ is given by

$$g'(u_j) = r'(u_j) * \cos(\theta(u_j)) - r(u_j) * \sin(\theta(u_j)) * \theta'(u_j) \tag{4.14}$$

Once the value of u is known, the coordinates of point (X_2, Y_2) are given by

$$X_2 = X_1 \tag{4.15}$$

$$Y_2 = r(u) * \sin(\theta(u)) \tag{4.16}$$

b) If $dY/dX < 0$:

Figure 4.3(b) shows a section of cam profile with positive slope. The geometric relationship between points

(X_o, Y_o) and (X_1, Y_1) can be expressed as

$$f(u) = (r(u) + \epsilon) * \cos(\theta(u)) - X_o = 0 \qquad (4.17)$$

Points (X_1, Y_1) and (X_2, Y_2) are related as follow:

$$g(u) = r(u) * \sin(\theta(u)) - Y_1 = 0 \qquad (4.18)$$

As was the case for a section with positive slope, data points for a section with negative slope are generated using a Newton-Raphson iteration to solve Equations (4.17) and (4.18).

The algorithm for tool path generation was used to generate NC code automatically. The code was then transferred to a tape and fed into the Pratt & Whitney Tapemate Series C NC machine to produce the cam.

2) Dwells

The function needed to represent dwell cycles is simple and in non-parametric form. In this thesis, the procedure for data point generation for dwell cycles is taken directly from [4].

4.1.2 Estimation of cutting time

In machining the cam profile, the number of turns in the tool path is a significant factor in estimating the cutting time. A series of tests was conducted on the Pratt

& Whitney NC machine to estimate the time required to make a turn [4]. The NC machine was programmed to travel along different paths of equal length but with different numbers of turns. These tests, which are fully described in [4], are summarized below.

The first path selected was along the sides of a square of side 4 inches as shown in Figure 4.4. The time taken by the tool to traverse the sides of the square for a total of 20 cycles was measured. Note that the tool is required to make 4 turns per cycle on this path and the length of the path is 16 inches per cycle.

In the next test, the tool was driven along a staircase path from corner 1 to corner 3, and back to corner 1 of the square, as shown in Figure 4.4. The tool was thus programmed to make 20 turns per cycle along this path, which also has a length of 16 inches per cycle. The total time required to travel 20 cycles on this path was also measured.

In subsequent tests, the tool was programmed to travel along the similar staircase paths, but with 40, 80 and 100 turns per cycle. The distance per cycle for all these paths was kept equal (16 inches per cycle), even though the number of turns for each path varied. The data recorded is reproduced in Table 2. Based on these results, the estimated time to make a turn is taken to be 0.4 seconds.

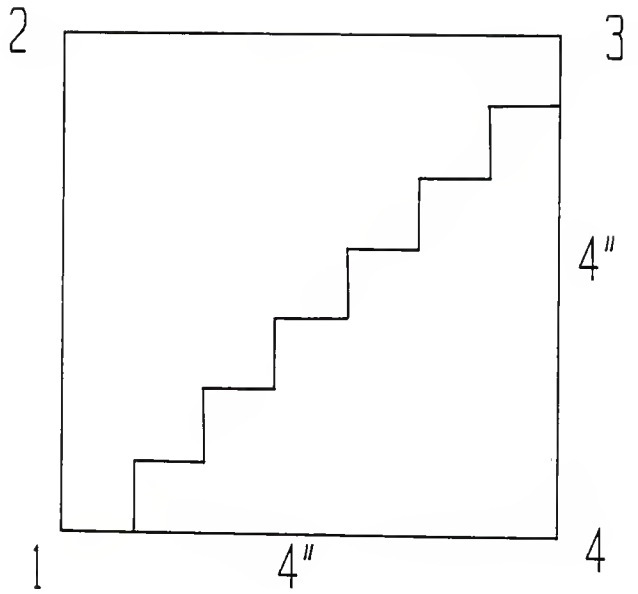

Figure 4.4 : Estimation of Time Lapse Per Turn in Tool Path
(Extracted from Reference [4])

Table 2 : Estimate of Time Lapse Per Turn

Case 1

No. of cycles	No. of turns/cycl	Total time (Min)
20	4	14.133
20	4	14.155

Case 2

Number of cycles	Number of turns/cycl	Total time(min)	Total time lapse(min)	Time lapse/turn
20	20	16.35	2.216	.33seconds
20	40	19.35	5.216	.39seconds
20	80	23.947	9.81	.37seconds
20	100	39.633	25.58	.38seconds

(Extracted form Reference [4])

Once the path generation has been completed, the distance the tool needs to travel to cut the cam profile can be computed as follows:

$$S_d = \sum_{i=0}^{n} [\ (Y_i - Y_{i-1})^2 + (X_i - X_{i-1})^2\ ]^{1/2} \qquad (4.19)$$

where

X_i is the x-coordinate of the data point "i"

Y_i is the y-coordinate of the data point "i"

n is the total number of steps

Now, the total time required to cut the cam can be estimated as

$$T_{cut} = S_d/Feed + 0.4 * N_t \qquad (4.20)$$

where

N_t is the total number of turns

Equation (4.20) is used as a cost function in the optimization process.

4.2 Cross-sectional Area of Cam

The material required to manufacture a cam is directly related to the cam volume. Assuming constant depth, the minimization of cam material is equivalent to the minimization of cam area.

In a previous chapter, we mentioned that the cam profiles of interest consist of a rise, a return, a top dwell and a bottom dwell. Therefore, the total cam area can be obtained by adding up the area of these zones.

$$A = A_1 + A_2 + A_3 + A_4 \tag{4.21}$$

where

A is the total cam area
A_1 is the area for the rise
A_2 is the area for the return
A_3 is the area for the top dwell
A_4 is the area for the bottom dwell

Equations for A_1, A_2, A_3 and A_4 are given as follows:

$$A_1 = \int_{\alpha_1}^{\beta_1} 0.5 * r^2(\theta)\, d\theta \tag{4.22}$$

$$A_2 = \int_{\alpha_1}^{\beta_1} 0.5 * r^2(\theta)\, d\theta \qquad (4.23)$$

$$A_3 = 0.5 * (R_o + L)^2 * \theta_t \qquad (4.24)$$

$$A_4 = 0.5 * R_o^2 * \theta_b \qquad (4.25)$$

where

$r(\theta)$ is the instantaneous radial distance to the cam profile

R_o is the base radius of cam

L is the total lift

α_1, β_1 are the bounds for rise and return zones

θ_t is the total angle for top dwell

θ_b is the total angle for bottom dwell

Converting equations (4.22) and (4.23) into the B-Spline form, we have

$$A_1 = \int_{u_o}^{u_1} 0.5 * r^2(u) * \theta'(u)\, du \qquad (4.26)$$

$$A_2 = \int_{u_o}^{u_1} 0.5 * r^2(u) * \theta'(u)\, du \qquad (4.27)$$

where

$r(u)$ is the instantaneous radial distance to the cam profile, given by Equation (4.5)

$\theta'(u)$ is the derivative of the angle of rotation, given by Equation (4.10)

The integrals in Equations (4.26) and (4.27) are evaluated numerically using Simpson's rule.

CHAPTER V

OPTIMIZATION

In engineering design applications, the goal of the designer is to produce the "best" design of the desired system or component. Numerical optimization is one of the tools that can be used to aid the designer in this endeavor.

In order to use optimization to solve a given problem, the problem must be stated in the following standard format:

Suppose the design of a system is specified by a vector b of r design variables:

$$\mathbf{b} = [\, b_1,\ b_2,\ b_3, \ldots,\ b_r]^T$$

Find the value of $\mathbf{b}$ to minimize a given cost function, $F(\mathbf{b})$, subject to the constraints

$$g_j(\mathbf{b}) \leq 0 \qquad j = 1,m$$

$$h_1(\mathbf{b}) = 0 \qquad 1 = 1,n$$

The optimization problem is fully defined once the set of design variables, cost and constraint functions are specified.

The optimal design procedure for solving this standard problem is by iterative improvement of the design vector, b. Each iteration of this solution process consists of three

distinct steps:

1) Analysis: In this step, the behavior of the system is analyzed at the current design. The cost and constraint functions are also evaluated at this step.

2) Design sensitivity analysis: The derivatives of the cost and constraint functions with respect to the design variables are computed at this step.

3) Design update: The cost and constraint function values from the system analysis are supplied to an optimization algorithm along with the design sensitivity information. The algorithm computes the required change in design and returns the updated design for the next iteration.

Implementing optimization techniques in cam design possesses several advantages over the conventional design approach. In optimization, once the standardized problem is formulated, they are several readily available nonlinear programming algorithms for solving the problem automatically [6, 7]. On the other hand, a conventional design approach is tedious and often requires a lot of repetitive work. As a result, implementing optimization techniques in cam design not only reduces the amount of designer time needed, but also reduces the level of skill required to produce the design.

In addition, optimization allows integration of design and manufacture. This will ensure that the final design satisfies both design and manufacturing requirements.

5.1 Choice of Design Variables

The first step in setting up an optimization model for a design problem is the selection of a set of design variables. The designer must carefully determine which parameters should be treated as design variables and which parameters should be kept constant. If the number of design variables is insufficient, the cost reduction may be limited, and in some cases, an acceptable design may be impossible to obtain. However, if the number of design variables is large, it will result in a more complex problem. The computer time required will also increase dramatically and the design problem may be too expensive to optimize.

In the formulation used in this thesis, we have selected the cam base radius, the orientation of the cam on the table of the NC machine, the offset of the roller follower and the coordinates of the control points of the rise and return B-splines as the design variables. These design variables are explained in more detail in the following sections.

1) The cam base radius

The cam base radius determines the size of cam. It is generally desirable to design a cam to be as small as possible. A small cam has several advantages; it occupies less space, it is cheaper to produce, and it reduces surface wear and torque [1]. In contrast, a large cam requires more space and is more expensive to produce.

However, if the size of the cam is too small, it may result in large pressure angles, high contact forces and stresses, and undercutting.

From the above discussion, it is obvious that the base radius of the cam should be considered as a design variable.

2) Offset Of The Roller Follower

From Equation (3.4), it is observed that the pressure angle is a function of the follower offset. During the rise, when the velocity Y' is positive, increasing offset reduces the pressure angle. However, increasing offset increases the pressure angle during the return, when Y' is negative. On the other hand, decreasing offset reduces the pressure angle on the return, but at the expense of an increased pressure angle during the rise. We consider offset as a design variable which is used to satisfy pressure angle requirements.

3) Orientation Of The Cam Blank

In Chapter IV, we discussed the procedure for variable step size path generation implemented in this thesis. The tool path is generated by alternately moving the tool along the x-axis and y-axis of the NC machine by varying distances. Since the steps generated for the cutter are along the machine axes, the pattern of steps generated is directly dependent on the orientation of the cam with respect to the machine axes. This orientation is measured as the angle between the x-axis of the NC machine and the line connecting the cam center of rotation and the starting point of the rise. For a fixed profile, varying this angle may change the total number of turns and the total length of the cutter path. Since these are key factors in determining the cutting time, the orientation of the cam blank will significantly influence the cutting time. Therefore, the angle defining the orientation of the blank is treated as a design variable.

Note that the orientation of the coordinates axis does not affect the feasibility of the design with respect to performance constraints. Also, this design variable is only applicable for the minimization of cam cutting time and not for the minimization of cam area.

4) The coordinates of the control points

As discussed in Chapter II, the shape of the cam profile is defined by a series of control points. The coordinates of the control points are treated as design variables in the optimization for the satisfaction of constraints and the reduction of cost. However, not all the coordinates can be used as design variables. Some of the coordinates may be determined uniquely by the specified boundary conditions. For example, the position boundary conditions of the rise determine the position of the first and the last points. Similarly, velocity boundary conditions at both ends decide the y-coordinates of the second and the second last control points. Higher derivative boundary conditions will have a similar effect on the control points as explained in Chapter II.

From the above discussion, the vector of design variables **b**, can be expressed as follows:

$$[\mathbf{b}] = [R_o,\ e,\ b_t,\ {}^pR_{1x},\ {}^pR_{2x},\ldots,\ {}^pR_{9x},\ {}^pR_{4y},\ {}^pR_{5y},\ {}^pR_{6y},\ {}^pr_{1x},\ {}^pr_{2x},\ldots,\ {}^pr_{9x},\ {}^pr_{4y},\ {}^pr_{5y},\ {}^pr_{6y}\ ]^T \qquad (5.1)$$

where

R_o is the base radius

e is the offset of roller follower

b_t is the orientation of the cam blank (This design variable is applicable only for the minimization of cutting time)

p^R_{ix} are the x-coordinates of the control points for the rise cycle

p^R_{jy} are the y-coordinates of the control points for the rise cycle

p^r_{ix} are the x-coordinates of the control points for the return cycle

p^r_{jy} are the y-coordinates of the control points for the return cycle

5.2 Cost

The minimization of a cost function is the main objective of optimization. We consider two different classes of minimization problems:

1) Minimize the cutting time: The objective of this minimization problem is to reduce the cutting time required to manufacture the cam. The equations used to estimate the cutting time are shown in Chapter IV.

2) Minimize the cam area: In many cases, the material cost is a more important factor than the machining time or

machining cost. In such cases, we consider the volume of material required to be the cost function. As discussed in Chapter IV, the volume of material required is directly proportional to the cross-sectional area of the cam. Therefore, the cam area is used as the cost function. The relevant equations for calculation of cam area are shown in Chapter IV.

5.3 Constraints

Defining a sufficient set of constraints is an important stage in optimal design. Constraints provide a means of preventing the optimization process from converging to an unacceptable solution. Therefore, the designer must study the system carefully, considering all performance requirements and restrictions, and then define constraints accordingly.

In this thesis, the constraints discussed below were imposed as standardized constraints for all problems. additional problem-dependent constraints can be added as needed.

1) Elimination of follower oscillation

The design of a cam is generally required to produce monotonic rise throughout the rise cycle, and monotonic descent throughout the return. Failure to satisfy these requirements results in follower oscillation during the motion. Oscillation can be avoided by restricting the velocity to be positive throughout the rise and negative throughout the return. These requirements can be enforced through the following set of constraints:

Rise Cycle:

$$g = - Y' \leq 0 \tag{5.2}$$

where

Y' is the reduced velocity of the follower

Referring to Equations (2.30), (2.31) and (2.36), Y' can be written as

$$Y' = \frac{L * \sum_{i=0}^{n} P_{iy} N_{i,k'}(u)}{\sum_{i=0}^{n} P_{ix} N_{i,k'}(u)} \tag{5.3}$$

where

L is the total lift

P_{ix} are the x-coordinates of the control points

P_{iy} are the y-coordinates of the control points

R_o is the base radius

$N_{i,k}(u)$ are the blending functions

$N_{i,k}'(u)$ are the first derivative of the blending functions

Return Cycle:

$$g = Y' \leq 0 \tag{5.4}$$

2) Pressure angle

To ensure a safe design, it is necessary to limit the maximum pressure angle to be within a specified range. This is enforced by the following constraint equation:

$$g = \phi^2 - \phi_d^2 \leq 0 \tag{5.5}$$

where

ϕ is the instantaneous pressure angle.

ϕ_d is the specified maximum pressure angle.

Substituting from Equation (3.4), the expanded form of the pressure angle constraint is given by

$$g = [\ \tan^{-1}\ (\ (Y' - e)/(a+Y)\ )\ ]^2 - \phi_d^2 \leq 0 \qquad (5.6)$$

where

e is the offset of the roller follower

a is the vertical distance from the cam axis to the base circle, given by Equation (3.3)

Y is the lift, given by Equation (2.28)

Y' is the reduced velocity, given by Equation (5.3)

3) Undercutting

The curvature of the cam profile must be adequate to ensure proper follower motion and to prevent excessive contact stress between the follower and the cam. This is achieved by restricting the cam curvature to be greater than one and a half times of the radius of the follower.

$$g = 1.5 * r_f - r_c \leq 0 \qquad (5.7)$$

where

r_f is the radius of the roller follower

r_c is the instantaneous radius of curvature of the cam profile

Substituting for the radius of curvature of the profile, we get

$$g = 1.5^* R_f - \frac{[\ C^2 + (Y' - e)^2\ ]^{3/2}}{C^2 + (Y' - e)(2Y' - e) - C^*Y''} \leq 0 \qquad (5.8)$$

where

C is the distance between the cam center and the profile, given by Equation (3.8)

Y'' is the reduced acceleration

Referring to Equations (2.30), (2.31), (2.32), (2.33) and (2.37), the reduced acceleration for a B-spline is

$$Y'' = \frac{\sum_{i=0}^{n} P_{ix}\, N_{i,k}'(u) \;^*\; L^* \sum_{i=0}^{n} P_{iy}\, N_{i,k}''(u)}{\left[\ \sum_{i=0}^{n} P_{ix}\, N_{i,k}'(u)\ \right]^3}$$

$$- \frac{L^* \sum_{i=0}^{n} P_{iy}\, N_{i,k}'(u) \;^*\; \sum_{i=0}^{n} P_{ix}\, N_{i,k}''(u)}{\left[\ \sum_{i=0}^{n} P_{ix}\, N_{i,k}'(u)\ \right]^3} \qquad (5.9)$$

4) Separation

Separation must be avoided to prevent unacceptable cam motions as well as other problems such as impact, noise, etc. This can be achieved by restricting the driving force to be positive throughout the motion:

$$g = - F_d \leq 0 \tag{5.10}$$

where F_d is the driving force, given by:

$$F_d = (P_L + M_f \ddot{Y}) / \cos(\phi) \tag{5.11}$$

where

P_L is the specified preload
M_f is the mass of the roller follower
$\ddot{Y}$ is the true acceleration

The true acceleration is given by

$$\ddot{Y} = Y'' * \omega^2 \tag{5.12}$$

where ω is the angular velocity of cam.

5) Contact Stress

Excessive stress in the region of contact between the cam and the follower can cause surface wear and failure of the cam system. This can be avoided by restricting the

$$g = S_c^2/S_d^2 - 1.0 \leq 0 \qquad (5.13)$$

where

S_c is the instantaneous contact stress, given by Equation (3.6)

S_d is the specified allowable stress

During the design process, it is important to ensure that the design satisfies all the specified constraints. Each rise and return zone is divided into equal intervals, and the checking of the constraints is done at the nodes between these intervals. Considering the computing time, the distance between two successive nodes must not be too small, otherwise the evaluation of constraint functions may be too expensive. However, if the interval is too large, it is possible to miss some violations. In this work, each rise zone and return zone is divided into 70 intervals. In a dwell zone, the value of all constraint functions is constant. Therefore, it is not necessary to divide the dwell zones into intervals to check for constraint violations. However, the behavior of constraints in a dwell zone is accounted for by evaluating the constraints at the boundaries of the rise zone and the return zone.

For other design problems, additional design constraints may be needed. In computer implementation of the method presented in this thesis, additional design constraints can be added conveniently through user supplied codes.

5.4 Optimization Method

After the optimal design problem is formulated, there are several algorithms available to solve the problem. One class of solution methods is called sequential unconstrained minimization techniques (SUMT). These methods find a solution to the constrained problem by solving a sequence of unconstrained problems. The sequence of solutions obtained for these unconstrained problems converges to the constrained solution [6]. This class of methods includes the exterior penalty function method described below.

The exterior penalty function method constructs the unconstrained problem of minimizing the following "pseudo-objective function" :

$$\Omega(\mathbf{b}, r_p) = F(\mathbf{b}) + r_p * P(\mathbf{b}) \qquad (5.14)$$

where

$F(\mathbf{b})$ is the original cost function

r_p is the penalty multiplier

$P(\mathbf{b})$ is the penalty function

The penalty function, $P(\mathbf{b})$ is given by

$$P(\mathbf{b}) = \sum_{j=1}^{m} \{ \max [0 , g_j(\mathbf{b})] \}^2 + \sum_{k=1}^{l} \{ h_k(\mathbf{b}) \}^2 \qquad (5.15)$$

where

$g_j(\mathbf{b})$ are the inequality constraints

$h_k(\mathbf{b})$ are the equality constraints

From Equations (5.14) and (5.15), we observe that a penalty is imposed if and only if one or more constraints are violated. When violations occur, the effect of the penalty multiplier is to magnify these violations and add them to the true cost, thus increasing the value of the pseudo-objective function. Therefore, the unconstrained optimization process will tend to move away from the infeasible regions, since constraint violations in the infeasible regions cause a significant increase in the pseudo-objective function value.

In order to avoid a numerically ill-conditioned problem, only a moderate value of the penalty multiplier is used in the initial optimization stages, and the value is increased as the optimization progresses.

For the minimization of cutting time, the cutting time is a discontinuous function of the design variables. This

is because the cutting time is dependent on the number of turns of the tool path. A small change in the value of a design variable may cause a step change in the number of turns. Therefore, a gradient-based method is not applicable for the minimization of cutting cost. Consequently, the unconstrained minimization method selected for cutting time minimization was a directed grid search [12]. This is a non-derivative method and is rather crude, but it performed satisfactorily in this case.

It is possible to implement derivative-based methods for minimization of cam area. This is because the partial derivatives of cam area and the constraint functions with respect to the design variables are continuous functions. The Fletcher-Reeves method [6] was used to perform the unconstrained minimization in this case. This method requires the first order partial derivatives of the pseudo-objective function with respect to the design variables:

$$\Omega'(\mathbf{b}) = F'(\mathbf{b}) + r_p * P'(\mathbf{b}) \qquad (5.16)$$

where

$\Omega'(\mathbf{b})$ is the first derivative of the pseudo-objective function

$F'(\mathbf{b})$ is the first derivative of the cost function

$P'(\mathbf{b})$ is the first derivative of the penalty function

P'(**b**) is given by

$$P'\mathbf{b}) = 2* \sum_{j=1}^{m} \max [\ 0\ ,\ g_j(\mathbf{b})\ ] * g_j'(\mathbf{b}) + \sum_{k=1}^{l} 2* h_k(\mathbf{b}) * h'_k(\mathbf{b}) \qquad (5.17)$$

where

$g_j'(\mathbf{b})$ are the first order partial derivatives of inequality constraints g_i with respect to the design variables, **b**

$h_k'(\mathbf{b})$ are the first order partial derivatives of the equality constraints h_k with respect to the design design variables, **b**

As shown in Equation (5.17), in order to use Fletcher-Reeves method, it is necessary to evaluate the first degree partial derivatives of the cost and constraint functions. The evaluation of these derivatives is discussed in Chapter VI.

CHAPTER VI

DESIGN SENSITIVITY ANALYSIS

In chapter V, it was stated that a gradient-based method is used for the minimization of cam area. The Fletcher-Reeves method selected for this work requires the evaluation of the derivatives of cost and constraint functions with respect to the design vector **b** defined in Equation (5.1).

The process of evaluating these derivatives is called "design sensitivity analysis" and is discussed in detail in this chapter. Only the derivation of non-zero derivatives is presented here. Any derivative that does not appear in the following discussion is a derivative with a constant value of zero.

6.1 Design Sensitivity Analysis of Constraints

1) Elimination of oscillation

Rise

$$g = - Y' \leq 0$$

$$\frac{\delta g}{\delta P_{ix}} = \frac{L * N_{i,k}'(u) * D_2}{D_1^2} \qquad i = 1,9 \qquad (6.1)$$

$$\frac{\delta g}{\delta P_{jy}} = - \frac{L * N_{j,k}'(u)}{D_1} \qquad j = 4,6 \qquad (6.2)$$

Where

$$D_2 = \sum_{i=0}^{n} P_{iy} N_{i,k}'(u) \qquad (6.3)$$

$$D_1 = \sum_{i=0}^{n} P_{ix} N_{i,k}'(u) \qquad (6.4)$$

Return

$$g = Y' \leq 0$$

$$\frac{\delta g}{\delta P_{ix}} = - \frac{L * N_{i,k}'(u) * D_2}{D_1^2} \qquad i = 1,9 \qquad (6.5)$$

$$\frac{\delta g}{\delta P_{jy}} = \frac{L * N_{j,k}'(u)}{D_1} \qquad j = 4,6 \qquad (6.6)$$

2) Pressure angle

$$g = \phi^2 - \phi_d^2 \leq 0$$

From equation (5.7), let

$$C = a + Y \tag{6.7}$$

$$V = (Y' - e)/C \tag{6.8}$$

The partial derivatives of g with respect to design variables are given in the following :

$$\frac{\delta g}{\delta R_o} = \frac{2 * \phi}{(1+V^2)} * \frac{\delta V}{\delta R_o} \tag{6.9}$$

$$\frac{\delta g}{\delta e} = \frac{2 * \phi}{(1+V^2)} * \frac{\delta V}{\delta e} \tag{6.10}$$

$$\frac{\delta g}{\delta P_{ix}} = \frac{2*\phi}{(1+V^2)} * \frac{\delta V}{\delta P_{ix}} \qquad i = 1,9 \tag{6.11}$$

$$\frac{\delta g}{\delta P_{jy}} = \frac{2*\phi}{(1+V^2)} * \frac{\delta V}{\delta P_{jy}} \qquad j = 4,6 \tag{6.12}$$

Where

$$\frac{\delta V}{\delta R_o} = \frac{(e - Y')}{C^2} * \frac{\delta C}{\delta R_o} \tag{6.13}$$

$$\frac{\delta V}{\delta e} = - \frac{[C + (Y'-e)]}{C^2} * \frac{\delta C}{\delta e} \tag{6.14}$$

$$\frac{\delta V}{\delta P_{ix}} = \frac{\delta Y'}{\delta P_{ix}} * \frac{1}{C} \tag{6.15}$$

$$\frac{\delta V}{\delta P_{jy}} = \left[C * \frac{\delta Y'}{\delta P_{jy}} - (Y' - e) * \frac{\delta C}{\delta P_{jy}} \right] * \frac{1}{C^2} \qquad (6.16)$$

$$\frac{\delta C}{\delta R_o} = \frac{R_o}{\text{sqrt}(R_o^2 - e^2)} \qquad (6.17)$$

$$\frac{\delta C}{\delta e} = - \frac{e}{\text{sqrt}(R_o^2 - e^2)} \qquad (6.18)$$

$$\frac{\delta C}{\delta P_{jy}} = L * N_{j,k}(u) \qquad (6.19)$$

$$\frac{\delta Y'}{\delta P_{ix}} = - \frac{L * N_{i,k'}(u) * D_2}{D_1^2} \qquad i= 1,9 \qquad (6.20)$$

$$\frac{\delta Y'}{\delta P_{jy}} = \frac{L * N_{j,k'}(u)}{D_1} \qquad j =4,6 \qquad (6.21)$$

3) Undercutting

$$g = 1.5 * r_f - r_c \leq 0$$

Referring to equation (5.9), let

$$N = [\ C^2 + (Y' - e)^2\ ]^{3/2} \qquad (6.22)$$

$$D = C^2 + (Y' - e)*(2Y' - e) - C*Y'' \qquad (6.23)$$

$$\frac{\delta g}{\delta R_o} = \frac{N * (2C - Y'') * \frac{\delta C}{\delta R_o} - 3C * \frac{\delta C}{\delta R_o} * [C^2 + (Y'-e)^2]^{1/2} * D}{D^2} \qquad (6.24)$$

$$\frac{\delta g}{\delta e} = \frac{N * \left[(2C - Y'') * \frac{\delta C}{\delta e} - 3 * Y' + 2 * e \right]}{D^2}$$

$$- \frac{3D * [C^2 + (Y'-e)^2]^{1/2} * \left[C * \frac{\delta C}{\delta e} - Y' + e \right]}{D^2} \qquad (6.25)$$

$$\frac{\delta g}{\delta P_{ix}} = \frac{N * \frac{\delta D}{\delta P_{ix}} - D * \frac{\delta N}{\delta P_{ix}}}{V^2} \qquad i = 1,9 \qquad (6.26)$$

Where

$$\frac{\delta N}{\delta P_{ix}} = 3 [C^2 + (Y' - e)^2]^{\frac{1}{2}} * (Y' - e) * \frac{\delta Y'}{\delta P_{ix}} \qquad (6.27)$$

$$\frac{\delta D}{\delta P_{ix}} = \frac{\delta Y'}{\delta P_{ix}} * (4Y' - 3e) - C * \frac{\delta Y''}{\delta P_{ix}} \qquad (6.28)$$

Where

$$\frac{\delta Y''}{\delta P_{ix}} = L * \left[D_1 * \frac{\delta N}{\delta P_{ix}} - 3*N* N_{i,k}'(u) \right] / (D_1{}^4) \qquad (6.29)$$

$$\frac{\delta g}{\delta P_{jy}} = \frac{N * \left[(2C - Y'') * \frac{\delta C}{\delta P_{jy}} + (4Y''-3e) * \frac{\delta Y'}{\delta P_{jy}} - C*\frac{\delta Y''}{\delta P_{jy}} \right]}{D^2}$$

$$- \frac{3D*[C^2 + (Y'-e)^2]^{1/2} * \left[C * \frac{\delta C}{\delta P_{jy}} + (Y' - e) * \frac{\delta Y'}{\delta P_{jy}} \right]}{D^2}$$

$$j = 4,6 \qquad (6.30)$$

Where

$$\frac{\delta Y''}{\delta P_{jy}} = \frac{L * [D_1 * N_{j,k}''(u) - E_1 * N_{j,k}'(u)]}{D_1{}^3} \qquad (6.31)$$

Where

$$E_1 = \sum_{i=0}^{n} P_{ix}\, N_{i,k}''(u) \qquad (6.32)$$

4) Separation

$$g = - F_d \leq 0$$

F_d is given by equation (5.10).

$$\frac{\delta g}{\delta R_o} = - \frac{(P_L + M_f \ddot{Y}) * \sin(\phi) * \frac{\delta \phi}{\delta R_o}}{\cos^2 \phi} \qquad (6.33)$$

$$\frac{\delta g}{\delta e} = - \frac{(P_L + M_f \ddot{Y}) * \sin(\phi) * \frac{\delta \phi}{\delta e}}{\cos^2 \phi} \qquad (6.34)$$

$$\frac{\delta g}{\delta P_{ix}} = - \frac{M_f w^2 * \cos(\phi) * \frac{\delta Y''}{\delta P_{ix}} + (P_L + M_f \ddot{Y}) * \sin(\phi) * \frac{\delta \phi}{\delta P_{ix}}}{\cos^2 \phi}$$

$$i = 1,9 \qquad (6.35)$$

$$\frac{\delta g}{\delta P_{jy}} = - \frac{M_f w^2 * \cos(\phi) * \frac{\delta Y''}{\delta P_{jy}} + (P_L + M_f \ddot{Y}) * \sin(\phi) * \frac{\delta \phi}{\delta P_{jy}}}{\cos^2 \phi}$$

$$j = 4,6 \qquad (6.36)$$

Referring to the design sensitivity analysis of pressure angle constraint, we have

$$\frac{\delta\phi}{\delta R_o} = \frac{\delta V}{\delta R_o} * \frac{1}{(1+V^2)} \qquad (6.37)$$

$$\frac{\delta\phi}{\delta e} = \frac{\delta V}{\delta e} * \frac{1}{(1+V^2)} \qquad (6.38)$$

$$\frac{\delta\phi}{\delta P_{ix}} = \frac{\delta V}{\delta P_{ix}} * \frac{1}{(1+V^2)} \qquad i = 1,9 \qquad (6.39)$$

$$\frac{\delta\phi}{\delta P_{jy}} = \frac{\delta V}{\delta P_{jy}} * \frac{1}{(1+V^2)} \qquad j = 4,6 \qquad (6.40)$$

5) Contact Stress

$$g = \frac{S_i^2}{S_d^2} - 1 \leq 0$$

Referring to equation (3.6), let

$$N = F_d * (r_c + r_f) \qquad (6.41)$$

$$D = \pi * t_c * r_f * r_c * [\ (1-\mu_c{}^2)/E_c + (1-\mu_f{}^2)/E_f\ ] \qquad (6.42)$$

$$D_k = \pi * t_c\ * r_c * [\ (1-\mu_c{}^2)/E_c + (1-\mu_f{}^2)/E_f\ ] \qquad (6.43)$$

$$\frac{\delta g}{\delta R_o} = \frac{1}{S_d{}^2} * \frac{\delta S_i{}^2}{\delta R_o} \qquad (6.44)$$

$$\frac{\delta g}{\delta e} = \frac{1}{S_d{}^2} * \frac{\delta S_i{}^2}{\delta e} \qquad (6.45)$$

$$\frac{\delta g}{\delta P_{ix}} = \frac{1}{S_d{}^2} * \frac{\delta S_i{}^2}{\delta P_{ix}} \qquad i = 1,9 \qquad (6.46)$$

$$\frac{\delta g}{\delta P_{jy}} = \frac{1}{S_d{}^2} * \frac{\delta S_i{}^2}{\delta P_{jy}} \qquad j = 4,6 \qquad (6.47)$$

Where

$$\frac{\delta S_i{}^2}{\delta R_o} = \frac{D\left[\ F_d * \frac{\delta r_c}{\delta R_o} + (r_c+r_f) * \frac{\delta F_d}{\delta R_o}\ \right] - N * \frac{\delta r_c}{\delta R_o} * D_k}{D^2} \qquad (6.48)$$

$$\frac{\delta S_i^2}{\delta e} = \frac{D\left[F_d * \frac{\delta r_c}{\delta e} + (r_c+r_f) * \frac{\delta F_d}{\delta e} \right] - N * \frac{\delta r_c}{\delta e} * D_k}{D^2} \qquad (6.49)$$

$$\frac{\delta S_i^2}{\delta P_{ix}} = \frac{D\left[F_d * \frac{\delta r_c}{\delta P_{ix}} + (r_c+r_f) * \frac{\delta F_d}{\delta P_{ix}} \right] - N * \frac{\delta r_c}{\delta P_{ix}} * D_k}{D^2} \qquad i = 1,9 \qquad (6.50)$$

$$\frac{\delta S_i^2}{\delta P_{jy}} = \frac{D\left[F_d * \frac{\delta r_c}{\delta P_{jy}} + (r_c+r_f) * \frac{\delta F_d}{\delta P_{jy}} \right] - N * \frac{\delta r_c}{\delta P_{jy}} * D_k}{D^2} \qquad j = 4,6 \qquad (6.51)$$

The partial derivatives of F_d, with respect to the design variables, can be obtained from the design sensitivity analysis of separation constraint.

$$\frac{\delta F_d}{\delta R_o} = \frac{(P_L + M_f \ddot{Y}) * \sin(\phi) * \frac{\delta \phi}{\delta R_o}}{\cos^2 \phi} \qquad (6.52)$$

$$\frac{\delta F_d}{\delta e} = \frac{(P_L + M_f \ddot{Y}) * \sin(\phi) * \frac{\delta \phi}{\delta e}}{\cos^2 \phi} \qquad (6.53)$$

$$\frac{\delta F_d}{\delta P_{ix}} = \frac{M_f \omega^2 * \cos(\phi) * \frac{\delta Y''}{\delta P_{ix}} + (P_L + M_f \ddot{Y}) * \sin(\phi) * \frac{\delta \phi}{\delta P_{ix}}}{\cos^2 \phi}$$

$$i = 1,9 \qquad (6.54)$$

$$\frac{\delta F_d}{\delta P_{jy}} = \frac{M_f \omega^2 * \cos(\phi) * \frac{\delta Y''}{\delta P_{jy}} + (P_L + M_f \ddot{Y}) * \sin(\phi) * \frac{\delta \phi}{\delta P_{jy}}}{\cos^2 \phi}$$

$$j = 4,6 \qquad (6.55)$$

From the design sensitivity analysis of undercutting constraint, we have

$$\frac{\delta r_c}{\delta R_o} = - \frac{N * (2C - Y'') * \frac{\delta C}{\delta R_o}}{D^2}$$

$$+ \frac{3C * \frac{\delta C}{\delta R_o} * [C^2 + (Y' - e)^2]^{1/2} * D}{D^2} \qquad (6.56)$$

$$\frac{\delta r_c}{\delta e} = -\frac{N * \left[(2C - Y'') * \frac{\delta C}{\delta e} - 3*Y' + 2*e \right]}{D^2}$$

$$+ \frac{3D*[C^2 + (Y'-e)^2]^{1/2} * \left[C * \frac{\delta C}{\delta e} - Y' + e \right]}{D^2}$$

(6.57)

$$\frac{\delta r_c}{\delta P_{ix}} = -\frac{N * \frac{\delta D}{\delta P_{ix}} - D * \frac{\delta N}{\delta P_{ix}}}{V^2} \qquad i= 1,9 \qquad (6.58)$$

$$\frac{\delta r_c}{\delta P_{jy}} = -\frac{N*\left[(2C - Y'') * \frac{\delta C}{\delta P_{jy}} + (4Y''-3e) * \frac{\delta Y'}{\delta P_{jy}} - C*\frac{\delta Y''}{\delta P_{jy}}\right]}{D^2}$$

$$+ \frac{3D*[C^2 + (Y'-e)^2]^{1/2} * \left[C * \frac{\delta C}{\delta P_{jy}} + (Y' - e) * \frac{\delta Y'}{\delta P_{jy}} \right]}{D^2}$$

$j= 4,6 \qquad (6.59)$

6.2 Design Sensitivity Analysis of Cost Function

Cam Area

The equations to evaluate cam area were given in Chapter IV. From those equations, the partial derivatives of the cam area with respect to the design variables can be derived as follows:

$$\frac{\delta A}{\delta R_o} = \int_{u_o}^{u_1} (R_o + L*Y) * D_1 \, du$$

$$+ R_o*\theta_b + (R_o+L)*\theta_t \qquad (6.60)$$

$$\frac{\delta A}{\delta P_{ix}} = 0.5 * \int_{u_o}^{u_1} (R_o + L*Y)^2 * N_{i,k}'(u) \, du$$

$$i = 1,9 \qquad (6.61)$$

$$\frac{\delta A}{\delta P_{jy}} = \int_{u_o}^{u_1} L * (R_o + L*Y) * N_{j,k}(u) * D_1 \, du$$

$$j = 4,6 \qquad (6.62)$$

CHAPTER VII

NUMERICAL EXAMPLES

The technique for cam design using B-spline curves as described in the preceding chapters was implemented in a computer program. Several numerical examples were solved to test the computer program and to verify the design technique developed in this work.

The physical properties for the material of cam and the follower were taken from [13]. These properties were kept unchanged in all the examples.

Physical Properties

Material: Hardened Steel SAE 1010 (for both cam & follower)
Density of the material = 0.28 lb/in^2
Young's modulus of elasticity = 29 x 10^6 psi
Poison's ratio = 0.29

7.1 Minimization of Cam Cutting Time

The machining data required for this problem was obtained from [10]. These parameters were also kept unchanged in all the examples presented in this chapter.

Machining Data:

Tool Material: High Speed Steel
Tool diameter = 0.75 inches
Number of teeth = 4
Cutting speed = 109.95 fpm
Feed per tooth = 0.0025 inch/tooth
Spindle speed = 560 RPM
Feed rate = 9.333 x 10^{-2} inch/sec

The first four examples presented here treat the cutting time as the cost function to be minimized. The design variables used in the cutting time minimization problems are given below:

Number of design variables = 27

B(1) : the base radius of the cam
B(2) : the offset of the roller follower
B(3) : the orientation of the blank on the NC table
B(4) : the x-coordinate of the second control point for the rise cycle.
B(5) : the x-coordinate of the third control point for the rise cycle.
B(6) : the x-coordinate of the fourth control point for the rise cycle.
B(7) : the x-coordinate of the fifth control point for the rise cycle.
B(8) : the y-coordinate of the fifth control point for the rise cycle.
B(9) : the x-coordinate of the sixth control point for the rise cycle.
B(10) : the y-coordinate of the sixth control point for the rise cycle.
B(11) : the x-coordinate of the seventh control point for the rise cycle.
B(12) : the y-coordinate of the seventh control point for the rise cycle.
B(13) : the x-coordinate of the eighth control point for the rise cycle.
B(14) : the x-coordinate of the ninth control point for the rise cycle.
B(15) : the x-coordinate of the tenth control point for the return cycle.
B(16) : the x-coordinate of the second control point for the return cycle.
B(17) : the x-coordinate of the third control point for the return cycle.
B(18) : the x-coordinate of the fourth control point for the return cycle.
B(19) : the x-coordinate of the fifth control point for the return cycle.
B(20) : the y-coordinate of the fifth control point for the return cycle.
B(21) : the x-coordinate of the sixth control point for the return cycle.

B(22) : the y-coordinate of the sixth control point for the return cycle.
B(23) : the x-coordinate of the seventh control point for the return cycle.
B(24) : the y-coordinate of the seventh control point for the return cycle.
B(25) : the x-coordinate of the eighth control point for the return cycle.
B(26) : the x-coordinate of the ninth control point for the return cycle.
B(27) : the x-coordinate of the tenth control point for the return cycle.

Example 1:

Preload = 320.0 lbs
Maximum allowable stress = 250,000 psi
Maximum allowable pressure angle = 25.0 degrees
Angular velocity of cam = 800 RPM
Mass of follower mechanism = 0.02 slugs
Lift = 1.0 inches
Cam thickness = 0.25 inches
Follower diameter = 0.85 inches
Follower thickness= 0.25 inches
Required accuracy on the profile = 0.01 inches

Cycle Characteristics:

Rise	Dwell	Return	Dwell
0.0-170.0	170.0-190.0	190.0-340.0	340.0-360.0

Design Variable	Initial Value	Final Value
B(1)	4.0000	3.6400
B(2)	0.0000	0.0500
B(3)	0.2094	0.7540
B(4)	0.4273	0.3827
B(5)	0.4987	0.4245
B(6)	0.5700	0.8668
B(7)	1.3532	1.0564
B(8)	0.1300	0.1000
B(9)	1.7805	1.4837
B(10)	0.6500	0.6700
B(11)	2.2655	1.8501
B(12)	0.9000	1.0000
B(13)	2.3460	2.2125
B(14)	2.4956	2.3621
B(15)	2.9308	2.4561
B(16)	3.8729	3.3230
B(17)	3.9211	3.3583
B(18)	3.9694	3.4458
B(19)	4.4970	4.4184
B(20)	1.0000	0.7700
B(21)	5.0253	5.0253
B(22)	0.3000	0.4700
B(23)	5.2653	5.2129
B(24)	0.1000	0.1400
B(25)	5.5053	5.4791
B(26)	5.7453	5.5489
B(27)	5.8653	5.7475

Comment

The design procedure started within the infeasible region with the maximum violation of 484.858 for the separation constraint. When the design stepped into the feasible region for the first time, the base radius and cutting time were found to be 5.80 inches and 1607.48 seconds respectively. Note that the jerk for the return cycle is actually started at zero as shown in Figure 7.2.

Maximum Values	Magnitude	Location On Cam Profile (degree)
Force	459.051 lbs	58.053
Pressure Angle	-16.863°	295.431
Contact Stress	1.708E+5 psi	58.053
Reduced Velocity	1.196 in/s	73.194
Reduced Acceleration	3.914 in/s^2	56.388
Reduced Jerk	-212.666 in/s^3	190.194

Highest constraint violation = 1.480 E-6

Total number of constraint violated = 1

Number of turns = 1530

Tool path distance = 33.00 inches

Cutting time = 965.55 seconds

% reduction in cutting time from the first feasible design = 39.93

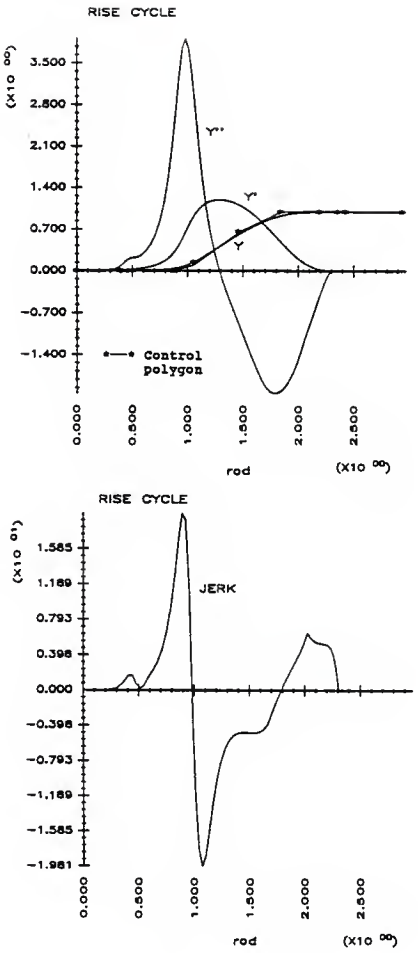

Figure 7.1 : Performance Characteristics for Example 1 (Rise Cycle)

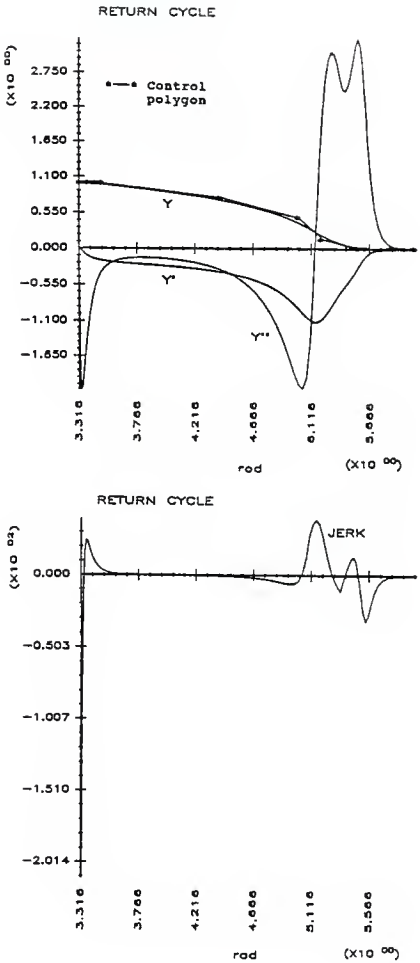

Figure 7.2 : Performance Characteristics for Example 1 (Return Cycle)

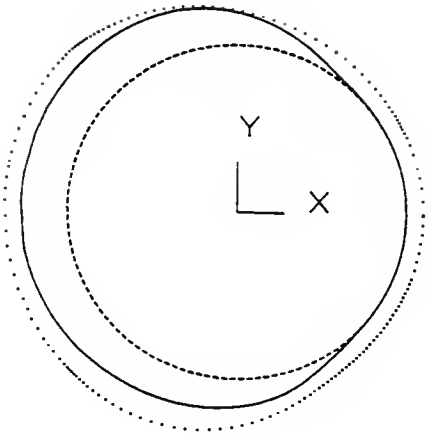

..... Cam profile of initial design
——— Cam profile of final design
- - - Base circle of final design

Figure 7.3 : Cam Profiles for Example 1

Example 2:

Preload = 370.0 lbs
Maximum allowable stress = 250,000 psi
Maximum allowable pressure angle = 25.0 degrees
Angular velocity of cam = 600 RPM
Mass of follower mechanism = 0.02 slugs
Lift = 1.3 inches
Cam thickness = 0.25 inches
Follower diameter = 0.85 inches
Follower thickness= 0.25 inches
Required accuracy on the profile = 0.01 inches

Cycle Characteristics:

Rise	Dwell	Return	Dwell
0.0-100.0	100.0-160.0	160.0-320.0	320.0-360.0

Design Variable	Initial Value	Final Value
B(1)	3.5000	5.2100
B(2)	0.0000	0.1000
B(3)	0.2094	0.0628
B(4)	0.2513	0.1641
B(5)	0.2933	0.2933
B(6)	0.3353	0.3528
B(7)	0.7960	0.6215
B(8)	0.1300	0.1200
B(9)	1.0473	0.8728
B(10)	0.6500	0.6600
B(11)	1.3327	1.1407
B(12)	0.9000	0.9100
B(13)	1.3800	1.3887
B(14)	1.4680	1.5465
B(15)	1.7240	1.6455
B(16)	3.3863	3.1210
B(17)	3.4379	3.1447
B(18)	3.4894	3.7687
B(19)	4.0521	4.0800
B(20)	1.0000	0.7000
B(21)	4.6156	4.5877
B(22)	0.3000	0.0900
B(23)	4.8716	4.8437
B(24)	0.1000	0.0000
B(25)	5.1760	5.1276
B(26)	5.3836	5.3836
B(27)	5.5116	5.5116

Comment

The design procedure started within the infeasible region with the maximum violation of 1722.565 for the undercutting constraint. The separation constraint was also violated with a maximum violation of 1354.038. When the design stepped into the feasible region for the first time, the base radius and cutting time were found to be 6.20 inches and 1699.40 seconds respectively.

Maximum Values	Magnitude	Location On Cam Profile (degree)
Force	497.570 lbs	33.972
Pressure Angle	19.557°	42.806
Contact Stress	1.541E+5 psi	36.908
Reduced Velocity	2.148 in/s	44.278
Reduced Acceleration	5.712 in/s^2	32.520
Reduced Jerk	-58.623 in/s^3	42.806

Highest constraint Violation = 0.000

Total number of constraint violated = 0

Number of turns = 2192

Tool path distance = 47.0 inches

Cutting time = 1381.24 seconds

% reduction in cutting time from the first feasible design = 18.72

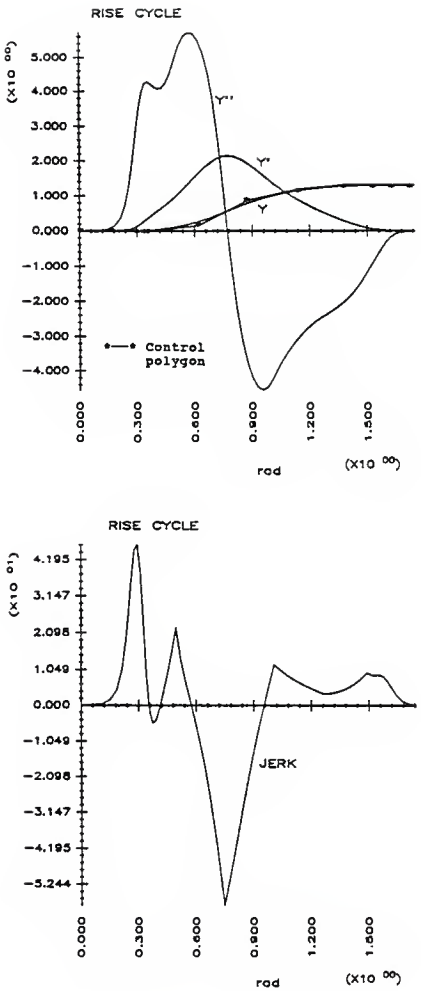

Figure 7.4 : Performance Characteristics for Example 2 (Rise Cycle)

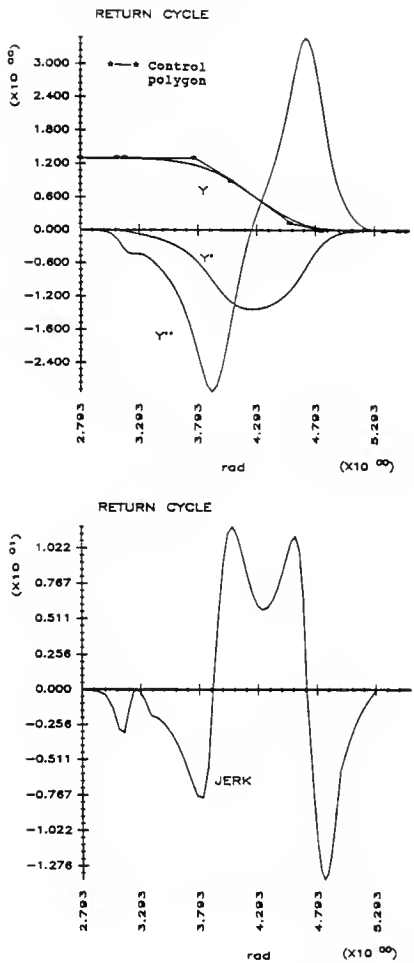

Figure 7.5 : Performance Characteristics for Example 2 (Return Cycle)

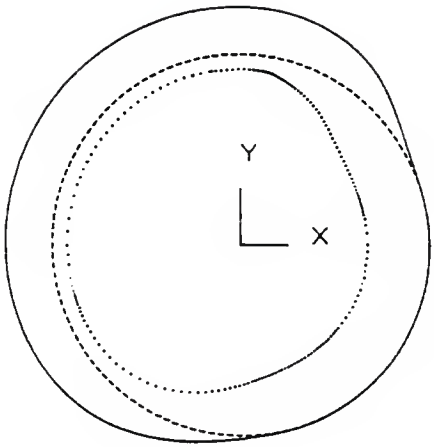

..... Cam profile of initial design
——— Cam profile of final design
- - - Base circle of final design

Figure 7.6 : Cam Profiles for Example 2

Example 3:

Preload = 380.0 lbs
Maximum allowable stress = 250,000 psi
Maximum allowable pressure angle = 28.0 degrees
Angular velocity of cam = 800 RPM
Mass of follower mechanism = 0.02 slugs
Lift = 1.2 inches
Cam thickness = 0.25 inches
Follower diameter = 0.85 inches
Follower thickness= 0.25 inches
Required accuracy on the profile = 0.01 inches

Cycle Characteristics:

Rise	Dwell	Return	Dwell
0.0-150.0	150.0-180.0	180.0-330.0	330.0-360.0

Design Variable	Initial Value	Final Value
B(1)	5.4000	5.2200
B(2)	0.0000	0.0500
B(3)	0.3491	0.9283
B(4)	0.3770	0.2592
B(5)	0.4400	0.2960
B(6)	0.5030	0.5292
B(7)	0.9322	0.9322
B(8)	0.1300	0.0000
B(9)	1.3092	1.3092
B(10)	0.8500	0.8500
B(11)	1.9990	1.9990
B(12)	1.0000	1.0000
B(13)	2.0700	2.2140
B(14)	2.3333	2.3400
B(15)	2.4551	2.4551
B(16)	3.5674	3.1878
B(17)	3.6151	3.2099
B(18)	3.7949	3.8211
B(19)	4.0606	4.3486
B(20)	0.9000	0.9900
B(21)	4.8507	4.8769
B(22)	0.2000	0.2900
B(23)	5.0907	5.0907
B(24)	0.1000	0.0000
B(25)	5.3307	5.3308
B(26)	5.5707	5.4268
B(27)	5.6908	5.5599

Comment

The design procedure started within the feasible region with an initial cutting time of 1531.54 seconds.

Maximum Values	Magnitude	Location On Cam Profile (degree)
Force	582.177 lbs	290.586
Pressure Angle	-15.798°	277.835
Contact Stress	1.664E+5 psi	290.586
Reduced Velocity	1.645 in/s	62.450
Reduced Acceleration	5.534 in/s^2	291.920
Reduced Jerk	34.261 in/s^3	284.866

Highest constraint violation = 2.004E-6

Total number of constraint violated = 1

Number of turn = 2196

Cutting time = 1377.60 seconds

Tool path distance = 46.59 inches

% Reduction in cutting time = 10.05

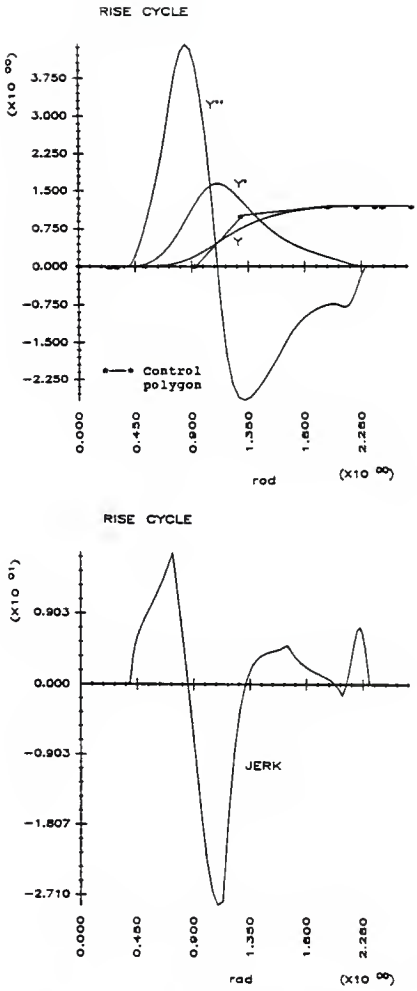

Figure 7.7 : Performance Characteristics for Example 3 (Rise Cycle)

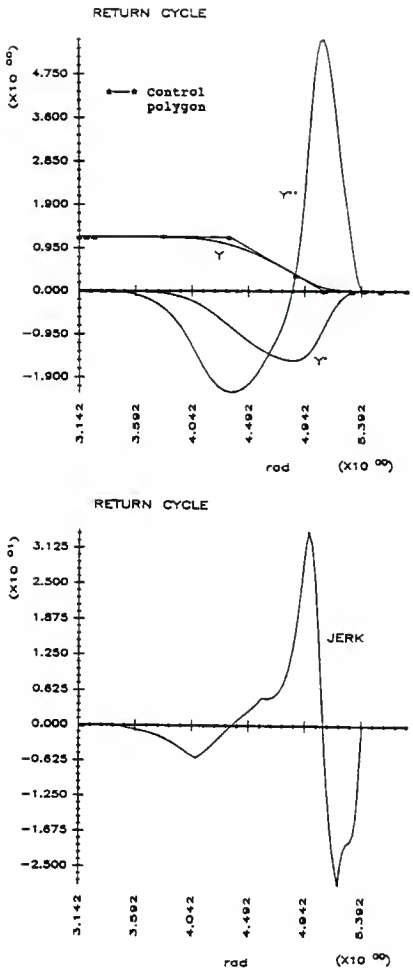

Figure 7.8 : Performance Characteristics for Example 3 (Return Cycle)

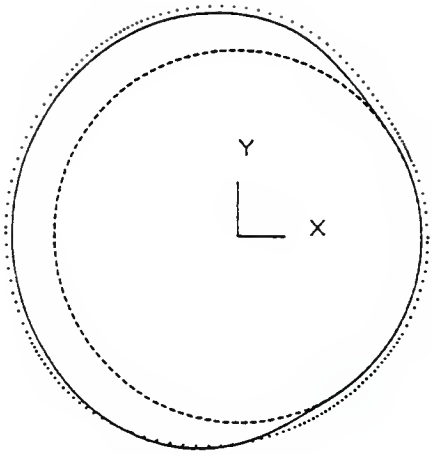

..... Cam profile of initial design
——— Cam profile of final design
- - - Base circle of final design

Figure 7.9 : Cam Profiles for Example 3

Example 4:

Preload = 400.0 lbs
Maximum allowable stress = 250,000 psi
Maximum allowable pressure angle = 20.0 degrees
Angular velocity of cam = 1000 RPM
Mass of follower mechanism = 0.02 slugs
Lift = 1.0 inches
Cam thickness = 0.25 inches
Follower diameter = 0.85 inches
Follower thickness= 0.25 inches
Required accuracy on the profile = 0.01 inches

Cycle Characteristics:

Rise	Dwell	Return	Dwell
-20.0-130.0	130.0-140.0	140.0-310.0	310.0-340.0

Design Variable	Initial Value	Final Value
B(1)	3.8000	2.4500
B(2)	0.0000	0.0000
B(3)	1.2566	1.3194
B(4)	0.0279	0.0279
B(5)	0.0909	0.1171
B(6)	0.4157	0.2063
B(7)	0.5831	0.6093
B(8)	0.1300	0.1300
B(9)	1.2219	1.2219
B(10)	0.9500	0.9500
B(11)	1.6499	1.7808
B(12)	1.0000	0.9600
B(13)	1.7209	1.8126
B(14)	1.8529	2.0754
B(15)	1.9751	2.1846
B(16)	2.7776	2.7776
B(17)	2.8324	2.8027
B(18)	2.8872	2.8872
B(19)	3.7817	3.4850
B(20)	0.9000	0.8900
B(21)	4.3805	4.3509
B(22)	0.3000	0.4800
B(23)	4.6525	4.6229
B(24)	0.0000	0.0700
B(25)	4.9245	4.9245
B(26)	5.1965	4.9444
B(27)	5.3325	5.0803

Comment

The design procedure started within the infeasible region with violations in undercutting, oscillation and stress constraints. The undercutting constraint was most violated with a maximum violation of 568.26. When the design stepped into the feasible region for the first time, the base radius and the cutting time were found to be equal to 4.7 inches and 1257.63 seconds respectively.

Maximum Values	Magnitude	Location On Cam Profile (degree)
Force	564.056 lbs	269.931
Pressure Angle	-19.521°	259.760
Contact Stress	1.653E+5 psi	266.744
Reduced Velocity	1.016 in/s	49.600
Reduced Acceleration	2.720 in/s^2	269.930
Reduced Jerk	-44.969 in/s^3	160.132

Highest constraint violation = 0.000000

Total number of constraint violated = 0

Number of turn = 1062

Cutting time = 676.57 seconds

Tool path distance = 23.49 inches

% reduction in cutting time from the first feasible design = 46.20

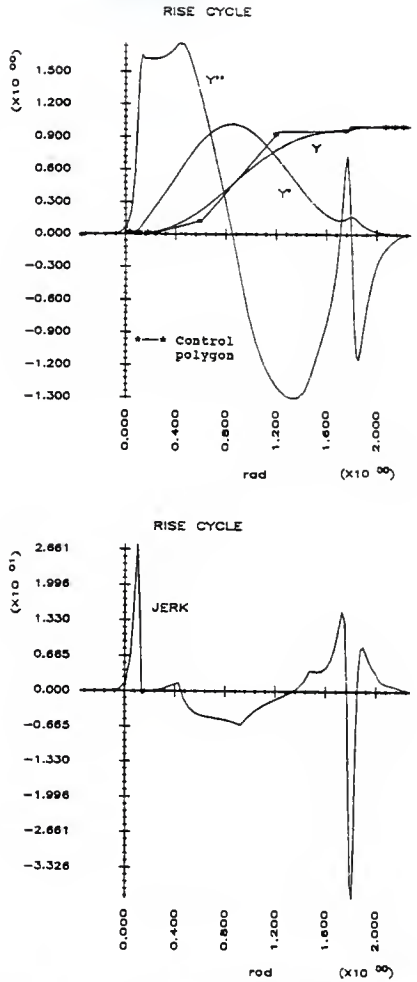

Figure 7.10 : Performance Characteristics for Example 4 (Rise Cycle)

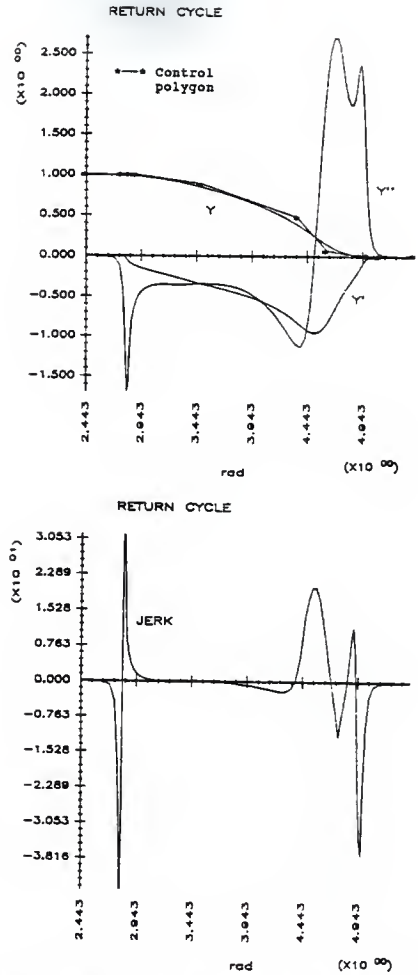

Figure 7.11 : Performance Characteristics for Example 4 (Return Cycle)

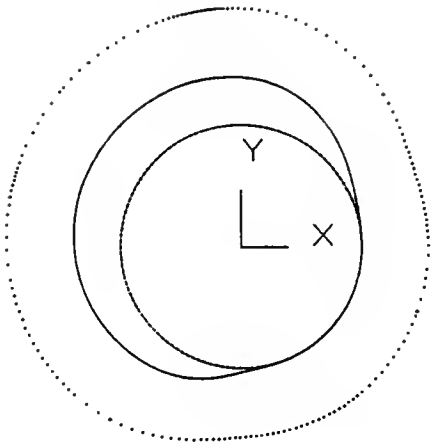

..... Cam profile of initial design
——— Cam profile of final design
- - - Base circle of final design

Figure 7.12 : Cam Profiles for Example 4

7.2 Minimization of Cam Material

The next three examples treat the cross-sectional area of the cam as the cost function to be minimized. The design variables for the minimization of cam material are given below:

Number of design variables = 26

B(1) : the base radius of the cam
B(2) : the offset of the roller follower
B(3) : the x-coordinate of the second control point for the rise cycle.
B(4) : the x-coordinate of the third control point for the rise cycle.
B(5) : the x-coordinate of the fourth control point for the rise cycle.
B(6) : the x-coordinate of the fifth control point for the rise cycle.
B(7) : the y-coordinate of the fifth control point for the rise cycle.
B(8) : the x-coordinate of the sixth control point for the rise cycle.
B(9) : the y-coordinate of the sixth control point for the rise cycle.
B(10) : the x-coordinate of the seventh control point for the rise cycle.
B(11) : the y-coordinate of the seventh control point for the rise cycle.
B(12) : the x-coordinate of the eighth control point for the rise cycle.
B(13) : the x-coordinate of the ninth control point for the rise cycle.
B(14) : the x-coordinate of the tenth control point for the return cycle.
B(15) : the x-coordinate of the second control point for the return cycle.
B(16) : the x-coordinate of the third control point for the return cycle.
B(17) : the x-coordinate of the fourth control point for the return cycle.
B(18) : the x-coordinate of the fifth control point for the return cycle.
B(19) : the y-coordinate of the fifth control point for the return cycle.

B(20) : the x-coordinate of the sixth control point for the return cycle.
B(21) : the y-coordinate of the sixth control point for the return cycle.
B(22) : the x-coordinate of the seventh control point for the return cycle.
B(23) : the y-coordinate of the seventh control point for the return cycle.
B(24) : the x-coordinate of the eighth control point for the return cycle.
B(25) : the x-coordinate of the ninth control point for the return cycle.
B(26) : the x-coordinate of the tenth control point for the return cycle.

Example 5:

Preload = 340.0 lbs
Maximum allowable stress = 250,000 psi
Maximum allowable pressure angle = 18.0 degrees
Angular velocity of cam = 800 RPM
Mass of follower mechanism = 0.02 slugs
Lift = 1.00 inches
Cam thickness = 0.25 inches
Follower diameter = 0.85 inches
Follower thickness= 0.25 inches

Cycle Characteristics:

Rise	Dwell	Return	Dwell
0.0-150.0	150.0-180.0	180.0-330.0	330.0-360.0

Design Variable	Initial Value	Final Value
B(1)	4.5000	3.7344
B(2)	0.0000	0.0001
B(3)	0.3770	0.3772
B(4)	0.4400	0.4424
B(5)	0.5030	0.5148
B(6)	1.1940	1.2282
B(7)	0.1300	0.0772
B(8)	1.5710	1.5945
B(9)	0.6500	0.6242
B(10)	1.9990	1.9231
B(11)	0.9000	0.9094
B(12)	2.0700	2.1345
B(13)	2.2020	2.2648
B(14)	2.5860	2.5848
B(15)	3.2860	3.2859
B(16)	3.3440	3.3433
B(17)	3.4020	3.3922
B(18)	4.0350	3.9976
B(19)	1.0000	0.9390
B(20)	4.4500	4.4062
B(21)	0.3000	0.2445
B(22)	4.9570	4.9349
B(23)	0.1000	0.0544
B(24)	5.2450	5.2382
B(25)	5.5330	5.5314
B(26)	5.6770	5.6768

Comment

The design procedure started within the feasible region with an initial area of 78.364 inches.

Maximum Values	Magnitude	Location On Cam Profile (degree)
Force	632.654 lbs	74.918
Pressure Angle	15.121°	88.806
Contact Stress	1.782E+5 psi	74.918
Reduced Velocity	1.153 in/s	88.806
Reduced Acceleration	-2.426 in/s^2	120.756
Reduced Jerk	-20.991 in/s^3	190.331

Highest constraint violation = 0.000000000

Total number of constraint violated = 0

Area = 55.493 inches

% reduction in area = 29.186

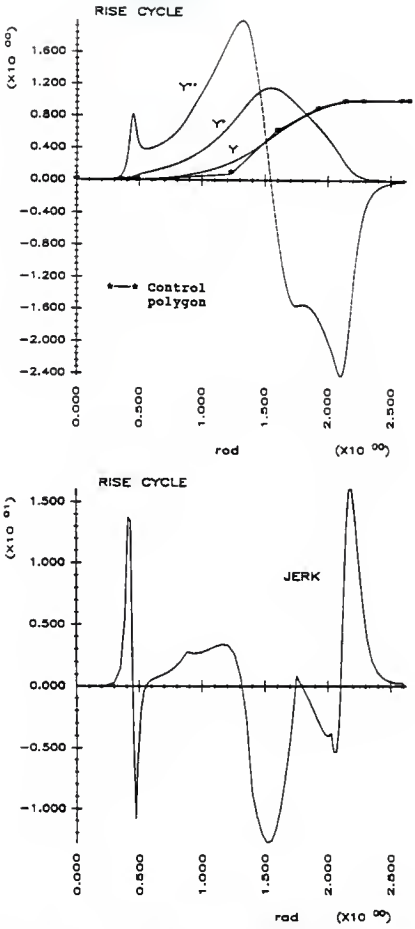

Figure 7.13 : Performance Characteristics for Example 5 (Rise Cycle)

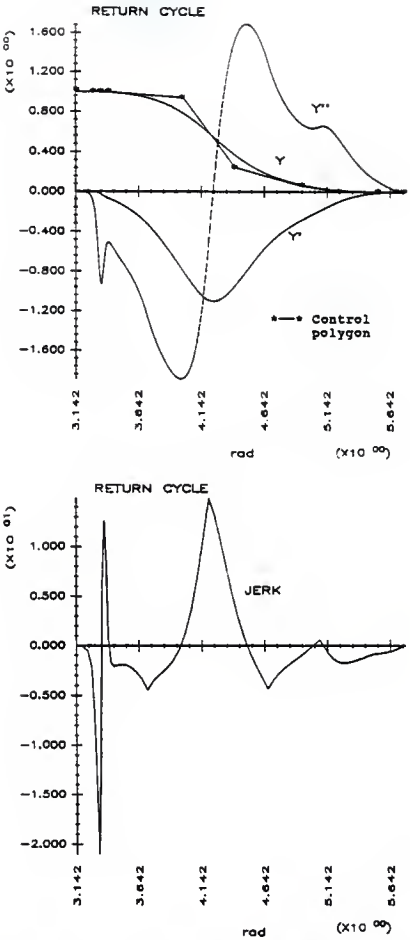

Figure 7.14 : Performance Characteristics for Example 5 (Return Cycle)

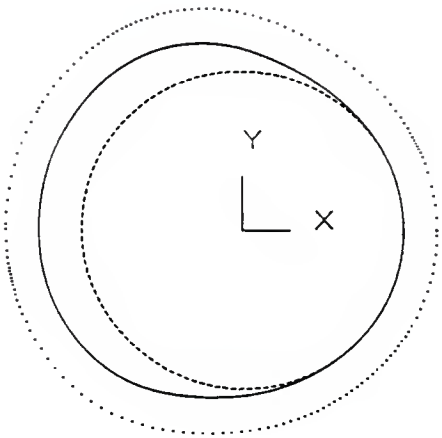

..... Cam profile of initial design
——— Cam profile of final design
- - - Base circle of final design

Figure 7.15 : Cam Profiles for Example 5

Example 6:

Preload = 360.0 lbs
Maximum allowable stress = 250,000 psi
Maximum allowable pressure angle = 25.0 degrees
Angular velocity of cam = 650 RPM
Mass of follower mechanism = 0.02 slugs
Lift = 1.50 inches
Cam thickness = 0.25 inches
Follower diameter = 0.85 inches
Follower thickness= 0.25 inches

Cycle Characteristics:

Rise	Dwell	Return	Dwell
180.0-310.0	310.0-340.0	-20.0-110.0	110.0-180.0

Design Variable	Initial Value	Final Value
B(1)	4.2000	3.7500
B(2)	0.0512	0.0516
B(3)	3.4683	3.4685
B(4)	3.5229	3.5248
B(5)	3.5775	3.5872
B(6)	4.1764	4.2050
B(7)	0.1300	0.0920
B(8)	4.4851	4.5204
B(9)	0.6675	0.6337
B(10)	4.7740	4.7953
B(11)	0.9411	0.9120
B(12)	4.9933	4.9998
B(13)	5.1116	5.1127
B(14)	5.3814	5.3818
B(15)	0.1334	0.1334
B(16)	0.1753	0.1746
B(17)	0.2172	0.2084
B(18)	0.6743	0.6416
B(19)	1.0000	0.9560
B(20)	1.1322	1.0947
B(21)	0.3000	0.2653
B(22)	1.3402	1.3218
B(23)	0.1000	0.0769
B(24)	1.5482	1.5427
B(25)	1.7562	1.7549
B(26)	1.8602	1.8600

Comment

The design procedure started within the infeasible region with an initial area of 81.868 inches. The separation constraint was violated with a maximum violation of 824.50. The oscillation constraint was also violated.

Maximum Values	Magnitude	Location On Cam Profile (degree)
Force	824.503 lbs	71.578
Pressure Angle	23.183°	253.083
Contact Stress	1.992E+5 psi	68.673
Reduced Velocity	2.002 in/s	256.732
Reduced Acceleration	4.373 in/s^2	71.578
Reduced Jerk	-86.491 in/s^3	9.505

Highest constraint violation = 4.307E-6

Total number of constraint violated = 1

Area = 67.373 inches

% reduction in area = 17.707

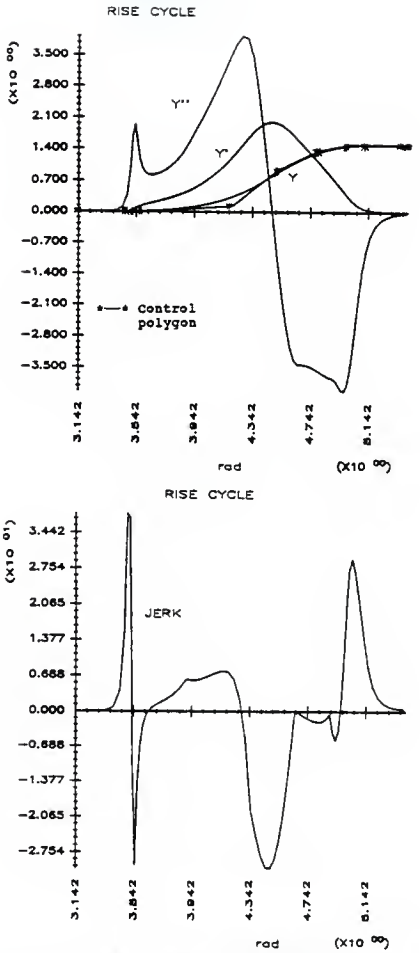

Figure 7.16 : Performance Characteristics for Example 6 (Rise Cycle)

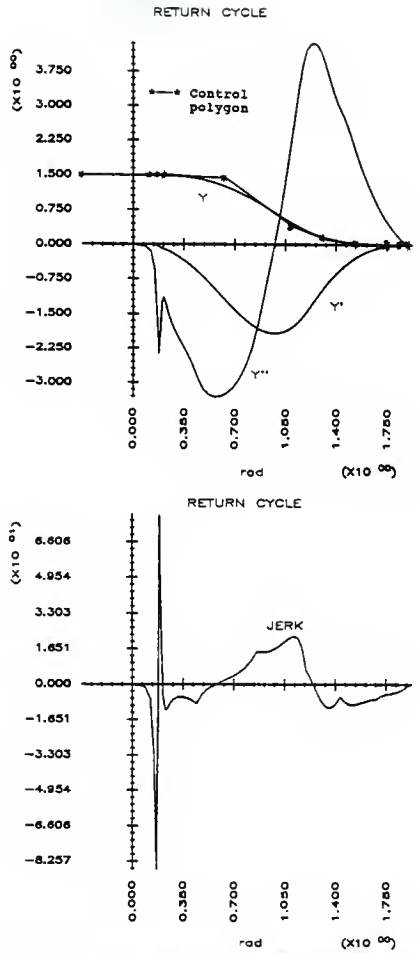

Figure 7.17 : Performance Characteristics for Example 6 (Return Cycle)

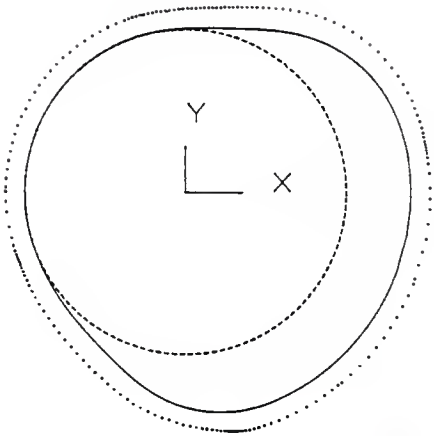

Figure 7.18 : Cam Profiles for Example 6

Example 7:

Preload = 360.0 lbs
Maximum allowable stress = 250,000 psi
Maximum allowable pressure angle = 20.0 degrees
Angular elocity of cam = 700 RPM
Mass of follower mechanism = 0.02 slugs
Lift = 1.10 inches
Cam thickness = 0.25 inches
Follower diameter = 0.85 inches
Follower thickness= 0.25 inches

Cycle Characteristics:

Rise	Dwell	Return	Dwell
0.0-140.0	140.0-150.0	150.0-330.0	330.0-360.0

Design Variable	Initial Value	Final Value
B(1)	5.0000	3.5655
B(2)	0.0000	0.0001
B(3)	0.3519	0.3523
B(4)	0.4107	0.4148
B(5)	0.4695	0.4918
B(6)	1.1144	1.1822
B(7)	0.1300	0.0301
B(8)	1.4484	1.5272
B(9)	0.6687	0.5940
B(10)	1.7657	1.7711
B(11)	0.9442	0.8981
B(12)	1.9896	2.0329
B(13)	2.1169	2.1459
B(14)	2.4122	2.4097
B(15)	3.2860	3.2858
B(16)	3.3440	3.3415
B(17)	3.4020	3.3794
B(18)	4.0350	3.9570
B(19)	1.0000	0.8614
B(20)	4.6690	4.5813
B(21)	0.3000	0.1865
B(22)	4.9570	4.9146
B(23)	0.1000	0.0208
B(24)	5.2450	5.2327
B(25)	5.5330	5.5302
B(26)	5.6770	5.6767

Comment

The design procedure started within the feasible region with an initial area of 99.742 inches.

Maximum Values	Magnitude	Location On Cam Profile (degree)
Force	699.396 lbs	76.552
Pressure Angle	20.153°	84.511
Contact Stress	1.861E+5 psi	76.552
Reduced Velocity	1.525 in/s	86.277
Reduced Acceleration	-3.324 in/s^2	191.603
Reduced Jerk	-93.409 in/s^3	190.698

Highest constraint violation = 2.134E-5

Total number of constraint violated = 2

Area = 54.017 inches

% reduction in area = 45.840

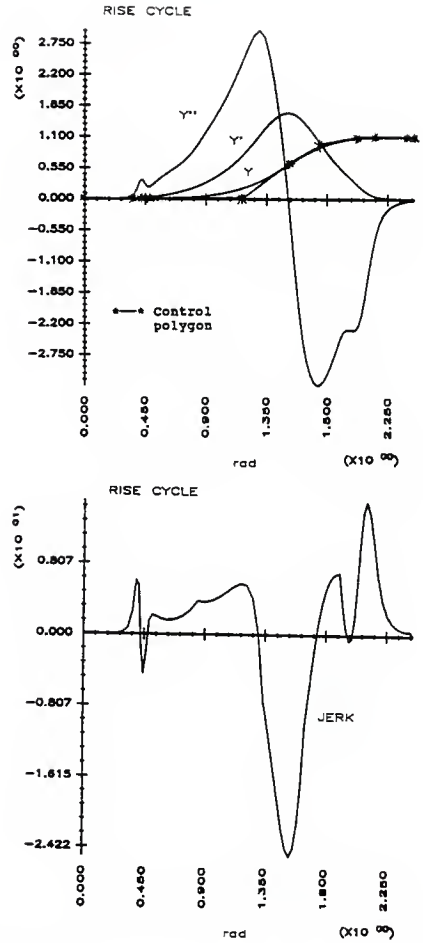

Figure 7.19 : Performance Characteristics for Example 7 (Rise Cycle)

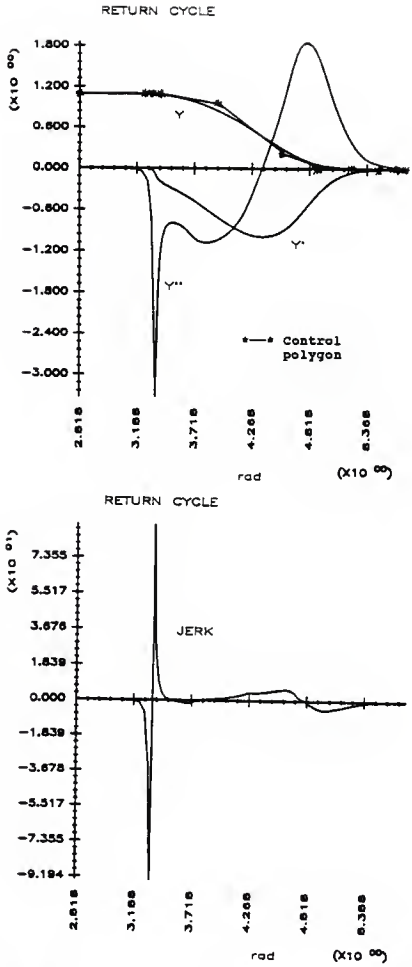

Figure 7.20 : Performance Characteristics for Example 7 (Return Cycle)

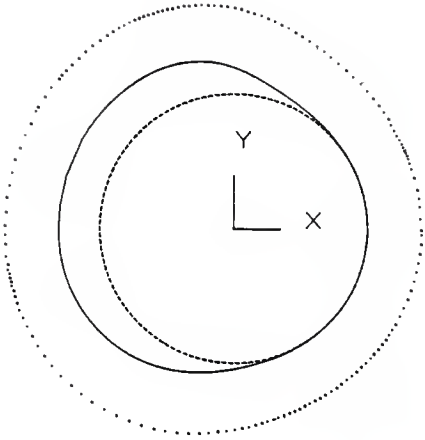

..... Cam profile of initial design
——— Cam profile of final design
- - - Base circle of final design

Figure 7.21 : Cam Profiles for Example 7

CHAPTER VIII

CONCLUSIONS

In this thesis, a new technique for designing plate cams has been developed. The approach adopted was to model the cam profile by B-spline curves, and use the B-spline representation in the design process. In addition to satisfying the boundary conditions, B-splines are capable of providing design control over the shape of the profile in the interior of a motion cycle, which is a crucial factor for satisfying the specified design requirements in this region. B-splines possess several attractive properties and can be used to model a large variety of complex curves that cannot be modeled by either the standard curves or the polynomials of the conventional design methods. Consequently, B-splines are capable of solving a large variety of problems and produce a wider range of solutions.

The integration of design and manufacture has also been considered for the case of plate cams. The objectives of considering the relevant manufacturing concerns is to produce a design which requires either minimum machining time or minimum material cost, in addition to satisfying the specified design requirements.

It is a tedious procedure to manually manipulate B-splines in parametric design because of the large number of design parameters involved. In order to overcome this difficulty, optimization techniques have been implemented to automate the design procedure.

The implementation of optimization techniques produced several distinct advantages. These techniques successfully solved the test problems with minimal user intervention, thus reducing the amount of designer time and the skill level required to produce the design. They also allow the designer to produce the best design with respect to the specified design objective and performance requirements.

Optimization techniques also allow the integration of design and manufacture. Integration is achieved by selecting the objective function based on the manufacturing concerns and the constraint functions based on the performance requirements that the design must satisfy. The objective function is either the machining time required for producing the cam on an NC machine or the material cost.

In the case of machining time minimization, a formulation to estimate the cutting time was derived based on a variable step size cutter path generation algorithm. In this case, the cutting time was used as the cost function. The minimization of material cost, assuming constant depth,

is equivalent to minimization of the cross-sectional area of the cam. In this case, the cross-sectional area is used as the cost function in the optimization process.

Several constraints were considered to ensure that the final design is safe and acceptable. The design requirements considered were limits on pressure angle and contact stress, along with elimination of separation, oscillation, and undercutting. Other design requirements can be conveniently included as desired through user-supplied constraint functions which can be input through user-supplied subroutines.

The set of design variables considered included the base radius of the cam, the offset of the roller follower, the orientation of the cam blank on the NC machine table, and the coordinates of the control points of the B-splines.

An exterior penalty function method was used to solve the optimization problems of both the minimization of machining time and the minimization of material cost. For the minimization of machining time, which is a discontinuous function, a directed grid search method is used to solve the unconstrained minimization sub-problem. For the minimization of material cost, where the cost and constraint functions are continuous, the Fletcher-Reeves conjugate-gradient method is used for unconstrained minimization.

Several numerical examples were solved to verify the proposed design technique. In all the examples, this technique was consistently effective in constraint correction and cost reduction. The design procedure was highly automated and required little designer intervention. The method was also very robust and able to handle a wide variety of problems, which indicates the great potential of B-splines and optimization techniques as design tools in cam design.

The work that has been done in this thesis offers several possibilities for future development. More work is needed to extend this technique to other types of cam and follower systems. It is also recommended that this technique be expanded to account for design problems involving cams with multiple rise cycles and/or multiple return cycles. Future efforts could also be directed towards treating the manufacturing aspects in greater detail. It is recommended that parameters such as feed, cutting speed, and tool diameter also be considered as design variables in the optimization. An exploration of different optimization techniques to improve the computational efficiency of the design process is also necessary for enhanced performance.

REFERENCES

1. Rothbart, Harold A., Cams - Design, Dynamics and Accuracy, John Wiley and Sons, Inc., 1956.

2. Tesar, Delbart and Mathew, Gary., The Dynamic Synthesis Analysis, and Design of Modeled Cam Systems, Lexington Books, 1976.

3. Shigley, J.E. and Uicker, J.J., Theory of Machines and Mechanisms, McGraw-Hill, 1980.

4. Husain, Farrukh Syed, "Computer Integrated Manufacture of Optimal Plate Cams", Master Thesis, Department of Mechanical Engineering, Kansas State University, 1987.

5. Sànchez, M. Nó and Jalón, J. García de, "Application of B-Spline Functions to the Motion Specifications of Cams," ASME pap. no. 80-DET-28, Oct. 1980.

6. Vanderplaats, G. N., Numerical Optimization Techniques for Engineering Design with Applications, McGraw-Hill, 1984.

7. Rao, S. S., Optimum Theory and Applications, Wiley Eastern Limited, 1978.

8. Mortenson, Michael E., Geometric Modeling, John Wiley & Sons, Inc., 1985.

9. Terauch, Yoshio and El Shakery, Sabry A., "A Computer Aided Method for Optimum Design of Plate Cam Size Avoiding Undercutting and Separation Phenomenon - I," Mechanism and Machine Theory, vol. 18, no. 2, 1983.

10. Metcut Research Associates, Inc., Machining Data Handbook, Machinability Data Center., 1972.

11. Vaithianathan, Raj., Manual for Numerical Control Machine.

12. Jones, R.E., MINA,. Sandia Labs; Library FxMath.

13. Mark's Standard Handbook for Mechanical Engineers, McGraw-Hill, 1978.

14. Pagel, Pulena A., "Sizing Cams for Long Life," Machine Design, vol. 50, no. 20, Sept 7 1978.

COMPUTER INTEGRATED MANUFACTURE OF OPTIMAL B-SPLINE CAMS

by

HOK SIN TEOH

B.S., Kansas State University, 1987

AN ABSTRACT OF A MASTER'S THESIS

submitted in partial fulfillment of the

requirements for the degree

MASTER OF SCIENCE

Department of Mechanical Engineering

KANSAS STATE UNIVERSITY
Manhattan, Kansas

1989

ABSTRACT

Conventional methods of designing cams are very restrictive and usually produce designs which only guarantee satisfaction of the boundary conditions. The standard curves and polynomials used in conventional design techniques do not provide control over the interior of a motion cycle; thus the design obtained may violate other design requirements such as pressure angle and stress limits. The primary objective of this thesis is to develop an automated design technique for plate cams which provides control over the entire profile of the cam. A second objective is to integrate the design and manufacture of plate cams in order to produce designs which not only satisfy the design requirements, but also ensure efficiency in manufacture. To achieve the first objective, B-spline curves are used to model the lift diagram, and thereby the cam profile. The shape of the interior of a B-spline is only partly determined by the boundary conditions. Thus, the curve can be designed to first fit the boundary conditions; the shape of the interior can then be modified to satisfy other requirements without affecting the curve at its end points. Generally, manual design of a B-spline is very difficult because of the large number of the design variables involved. To overcome this difficulty, a design technique based on nonlinear optimization is developed for the purpose of automating the design process. Optimization also allows the designer to produce the best design for a problem with respect to the specified requirements. In addition, optimization techniques allow the integration of design and manufacture by permitting requirements from both aspects to be included in the optimization process. Two classes of problems are considered in this thesis: design for minimum machining time and design for minimum material cost. In both cases, the optimization problems are solved by an exterior penalty function method. For the minimization of machining time, which is a discontinuous function, a directed grid search method is used to solve the unconstrained minimization subproblem. For the minimization of material cost, where the cost and constraint functions are continuous, the Fletcher-Reeves conjugate-gradient method is used for unconstrained minimization. The design technique developed in this thesis was implemented in a computer program and tested on several examples. In all the examples, the design technique produced good designs very effectively. The design process was also found to be highly automated and required very little designer intervention. It may be concluded that B-splines are a powerful tool for plate cam design and that the proposed optimization technique is a reliable, robust, and computationally viable method for automated design of B-spline cams.